

T.C.

YEDİTEPE UNIVERSITY

INSTITUTE OF HEALTH SCIENCES

DEPARTMENT OF PHYSIOLOGY

**THE EFFECTS OF SOCIAL AND PHYSICAL
ENRICHED ENVIRONMENT ON SENSORIMOTOR
AND SOCIAL PERFORMANCE IN A
CEREBELLAR INFARCT MICE MODEL**

MASTER THESIS

AYTEN KARDAŞ, PT

İSTANBUL

2024

T.C.

YEDİTEPE UNIVERSITY

INSTITUTE OF HEALTH SCIENCES

DEPARTMENT OF PHYSIOLOGY

**THE EFFECTS OF SOCIAL AND PHYSICAL
ENRICHED ENVIRONMENT ON SENSORIMOTOR
AND SOCIAL PERFORMANCE IN A
CEREBELLAR INFARCT MICE MODEL**

MASTER THESIS

AYTEN KARDAŞ, PT

SUPERVISOR

Prof. Dr. BAYRAM YILMAZ

CO- SUPERVISOR

Dr. YAVUZ YAVUZ

İSTANBUL

2024

THESIS APPROVAL FORM

Institute : Yeditepe University Institute of Health Sciences

Programme : Master in Physiology

Title of the Thesis : The Effects of Social and Physical Enriched Environment on Sensorimotor and Social Performance in a Cerebellar Infarct Mice Model

Owner of the Thesis : Ayten KARDAŞ

Examination Date : 07.05.2024

This study have approved as a Master Thesis in regard to content and quality by the Jury.

	Title, Name-Surname (Institution)
Chair of the Jury:	Prof. Dr. Bayram Yılmaz (Yeditepe University, Faculty of Medicine, Department of Physiology)
Supervisor:	Prof. Dr. Bayram Yılmaz (Yeditepe University, Faculty of Medicine, Department of Physiology)
Member/Examiner:	Prof. Dr. Burcu Gemici Başol (Yeditepe University, Faculty of Medicine, Department of Physiology)
Member/Examiner:	Doç. Dr. Mustafa Çağlar Beker (Istanbul Medeniyet University, Faculty of Medicine, Department of Physiology)

APPROVAL

This thesis has been deemed by the jury in accordance with the relevant articles of Yeditepe University Graduate Education and Examinations Regulation and has been approved by Administrative Board of Institute with decision dated and numbered

Prof. Dr. Bayram YILMAZ

Director of Institute of Health Sciences

DECLARATION

I hereby declare that all the information and documents in this study have been obtained in accordance with academic rules, and that all visual, auditory, and written data and results have been presented in compliance with scientific ethical principles. I affirm that I have not falsified any data used and have cited all the sources in accordance with scientific norms. Except for the cited sources, this thesis is original, produced under the supervision of Prof. Dr. Bayram Yılmaz, and written in accordance with the Thesis Writing Guidelines of the Institute of Health Sciences at Yeditepe University.



Ayten KARDAŞ

ACKNOWLEDGEMENTS

First of all, I would like to thank my esteemed supervisor, Prof. Dr. Bayram YILMAZ, who provided me with an invaluable opportunity to carry out my dream research, never spared his understanding and patience throughout this process, and always offered opportunities beyond the standards by enabling me to participate in both national and international platforms, thus supporting the development of my academic career.

I would like to extend my gratitude to all the faculty members of Yeditepe University Faculty of Medicine, especially Prof. Dr. Mehtap KAÇAR and Prof. Dr. Burcu GEMİCİ BAŞOL from the Department of Physiology, whose invaluable advice and guidance were always available whenever I needed them, and who supported me in every aspect with patience.

I would like to thank Dr. Yavuz YAVUZ and Dr. Sanem Aslihan AYKAN, who have been my greatest fortune in my academic life and the best mentors I could ever ask for. Their constant trust in me throughout this process has been a great source of motivation.

I would like to especially thank Habibe GÖREN and Zehra YAĞMUR EROL for their generous motivation, their sincere friendship, and for always being there for me whenever I needed them.

I would like to thank Dr. Cihan Süleyman Erdoğan for his incredible patience and for always finding solutions to every problem I encountered, as well as for his constant support.

I would like to thank Dr. Özge BAŞER, Dr. Buğra ÖZGÜN, Deniz ÖZEN, Yunus KOSİF, Cansu YAKIN and Buse Nur BOLAT for generously sharing their invaluable knowledge and expertise with me.

I would like to thank Dr. B. Tuvana US, Meltem YALÇIN OĞUZ, and Deniz ÖZLÜER for their constant support and incredible patience throughout this process.

Finally, endless thanks to my dear family: my father Aydın KARDAŞ, my mother Keziban KARDAŞ, and my brother Murat KARDAŞ, who have always been by my side with their trust, unconditional support, unending love, and understanding throughout my graduate education and my entire life. I also extend my heartfelt gratitude to my dear friend Anıl YÜCEER, who has always been there for me.

CONTENTS

THESIS APPROVAL FORM	ii
DECLARATION	iii
ACKNOWLEDGEMENTS.....	iv
ABSTRACT	xii
ÖZET	xiii
INTRODUCTION and PURPOSE.....	1
2. GENERAL INFORMATION.....	3
2.1. Cerebellum	3
2.1.1 Anatomy and Organization of the Cerebellum	3
2.1.2. Function and Functional Map of the Cerebellum.....	4
2.2. Cerebellar Infarct	8
2.2.1 Pathophysiology	8
2.2.2. Epidemiology and Clinical Findings	9
2.2.3. Prognosis	10
2.2.4. Treatment.....	10
2.3 Enriched Environment.....	11
2.4 Biorientation Defective 1	12
3. MATERIALS AND METHODS	14
3.1. Experimental Animals	14
3.2. Mouse Production Strategy.....	14
3.3. Experimental Groups	14
3.3.1 Sham Group.....	15
3.3.2. Standard Environmental Condition (STD) Group.....	15
3.3.3. Physical Enrichment (PE) Group	16
3.3.3. Enriched Enrichment (EE) Group	17
3.3.5. Enriched Enrichment+3 Healthy Mice (EE+3) Group.....	17
3.4. Cerebellar Infarction Modelling	18
3.5. Sensorimotor and Social Performance Assessment.....	19
3.5.1. Footprint Test.....	19
3.5.2. Wire Walk Test.....	22
3.5.3. Three Chamber Test.....	23
3.6. Cardiac Perfusion and Brain Slicing	25
3.7. Hematoxylin And Eosin Staining and Visualization.....	26
3.8. Immunofluorescence Staining for Biorientation Defective 1.....	27
3.9. Statistical Analysis	28

4. RESULTS.....	29
4.1. Sensorimotor and Social Performance Assessment Results	29
4.1.1 Footprint Analysis	29
4.1.2. Wire Walk Test Analysis.....	39
4.1.3. Three Chamber Test Analysis	43
4.1.4. H&E Staining Findings.....	44
4.1.5 BOD1 Immunofluorescence Staining Findings.....	45
5. DISCUSSION.....	46
6. REFERENCES.....	52



LIST OF TABLES

Table 1. Footprint Test Results	38
Table 2. Wire Walk Test Results	43



LIST OF FIGURES

Figure 1. Schematic diagram of the lobes and lobules of the cerebellar cortex (19).....	4
Figure 2. Somatotopic representations of cerebellum (22).....	6
Figure 3. a Cerebellar task activation maps and resting-state networks. b Cerebellar functional gradients. c Relationship of functional gradients 1 and 2 with task activation maps and resting-state networks (34).	8
Figure 4. Schematic illustration how BOD1 regulates the cerebellar IV/V lobe Purkinje cells and their interaction with the FNCaMKII α + circuit that is associated with motor coordination (61).....	13
Figure 5. Experimental groups.....	14
Figure 6. The Study Design for the Sham Group.	15
Figure 7. The Study Design for the STD group.....	16
Figure 8. The Study Design for the PE group.....	16
Figure 9. The Study Design for the EE group.	17
Figure 10. The Study Design for the EE+3 group.	18
Figure 11. Stereotaxic Operation and Coordinates	19
Figure 12. Footprint Sheet. The red arrows represent the step lengths, with A showing the right front, B indicating the left front, C illustrating the right hind, and D demonstrating the left hind.	20
Figure 13. Footprint Sheet. The red arrows represent the step width. E represents the step width of the front paws, while F represents the step width of the hind paws.....	21
Figure 14. Footprint Sheet. The red arrows indicate the step overlap distance. G represents the right side, while H represents the left side.....	21
Figure 15. The Wire Walk Test Design.....	22
Figure 16. Moments from the video of the wire walk test: Picture A provides a bottom-up view, while Picture B offers a side view.	23
Figure 17. Three-Chamber Sociability and Social Novelty Preference Test. A sociability. B social novelty preference.....	24
Figure 18. Schematic Representation of Cardiac Perfusion and Brain Slicing	26
Figure 19. H&E staining procedure and visualization.....	26
Figure 20. Image of cerebellum tissue post h&e staining captured at 20x magnification using TEM	27

Figure 21. Immunofluorescence Staining procedure for BOD1	27
Figure 22. Right hind step lengths across experimental groups in the footprint test analysis. Two Way repeated measure ANOVA TUKEY's multiple comparison test, *** p<0,001, ** p<0,01, * p<0,05.....	29
Figure 23. Left hind step lengths across experimental groups in the footprint test analysis. Two Way repeated measure ANOVA TUKEY's multiple comparison test, *** p<0,001, ** p<0,01, * p<0,05	30
Figure 24. Right front step lengths across experimental groups in the footprint test analysis. Two Way repeated measure ANOVA TUKEY's multiple comparison test, *** p<0,001, ** p<0,01, * p<0,05.....	31
Figure 25. Left front step lengths across experimental groups in the footprint test analysis. Two Way repeated measure ANOVA TUKEY's multiple comparison test, *** p<0,001, ** p<0,01, * p<0,05	33
Figure 26. Hind step width across experimental groups in the footprint test analysis. Two Way repeated measure ANOVA TUKEY's multiple comparison test, *** p<0,001, ** p<0,01, * p<0,05.....	34
Figure 27. Front step width across experimental groups in the footprint test analysis. Two Way repeated measure ANOVA TUKEY's multiple comparison test, *** p<0,001, ** p<0,01, * p<0,05.....	35
Figure 28. The right steps overlap distance across experimental groups in the footprint test analysis. Two Way repeated measure ANOVA TUKEY's multiple comparison test, *** p<0,001, ** p<0,01, * p<0,05.....	36
Figure 29. The left steps overlap distance across experimental groups in the footprint test analysis. Two Way repeated measure ANOVA TUKEY's multiple comparison test, *** p<0,001, ** p<0,01, * p<0,05.....	37
Figure 30. The right front foot fault across experimental groups in the wire walk test analysis. Two Way repeated measure ANOVA TUKEY's multiple comparison test, *** p<0,001, ** p<0,01, * p<0,05.....	39
Figure 31. The left front foot fault across experimental groups in the wire walk test analysis. Two Way repeated measure ANOVA TUKEY's multiple comparison test, *** p<0,001, ** p<0,01, * p<0,05.....	40
Figure 32. The right hind foot fault across experimental groups in the wire walk test analysis. Two Way repeated measure ANOVA TUKEY's multiple comparison test, *** p<0,001, ** p<0,01, * p<0,05.....	41

Figure 33. The left hind foot fault across experimental groups in the wire walk test analysis. Two Way repeated measure ANOVA TUKEY's multiple comparison test, *** p<0,001, ** p<0,01, * p<0,05.....	42
Figure 34. Social Preference Index. Two Way repeated measure ANOVA TUKEY's multiple comparison test, *** p<0,001, ** p<0,01, * p<0,05.	43
Figure 35. Social Novelty Preference Index. Two Way repeated measure ANOVA TUKEY's multiple comparison test, *** p<0,001, ** p<0,01, * p<0,05.....	44
Figure 36. A represents a detailed modeling of CI using the H&E staining technique. B , on the other hand, provides an illustration of the target region of the cerebellum, detailed with a Reference Brain Section image obtained from the Brain Allen Atlas (68).....	45
Figure 37. BOD1 immunofluorescence staining findings. Red arrows indicate regions with increased expression.	45

LIST OF ABBREVIATIONS

AICA	Anterior Inferior Cerebellar Artery
BOD1	Biorientation Defective 1
CI	Cerebellar Infarction
EE	Enriched Environment
EE+3	Enriched environment Plus 3 Healthy Mice
fMRI	Functional Magnetic Resonance Imaging
MRI	Magnetic Resonance Imaging
PE	Physical Enrichment
SNPI	The Social Novelty Preference Index
SPI	Social Preference Index
STD	Standard Environment
S1	Stranger Mouse 1
S2	Stranger Mouse 2
PICA	Posterior Inferior Cerebellar Artery
SCA	Superior Cerebellar Artery
TEM	Transmission Electron Microscopy

ABSTRACT

Ayten, K. (2024) The Effects of Social and Physical Enriched Environment on Sensorimotor and Social Performance in a Cerebellar Infarct Mice Model. Yeditepe University, Institute of Health Sciences, Department of Physiology, MSc thesis, İstanbul.

Cerebellar infarction (CI), a rare type of stroke can result in significant motor deficits such as ataxia and gait disorders, impacting daily activities and self-care, potentially leading individuals to experience social isolation. The present study aims to investigate effects of enriched environments as a therapeutic approach for CI in mice, assessing the influence of different environmental factors on the condition. Forty male C57BL/6 mice were divided into 5 groups: physical enrichment, enriched environment, enriched environment +3 healthy mice, standard housing, and sham. The CI model was induced in mice via stereotaxic injection of N5-(1-iminoethyl)-L-ornithine dihydrochloride. Sensorimotor and social performance were assessed pre-infarct and on specific days post-infarct using the wire walk test, footprint test, and three-chamber test. The infarct area was identified by Hematoxylin & Eosin staining. Immunohistochemistry was employed to visualize Biorientation Defective 1 (BOD1), a factor associated with motor coordination, utilizing a confocal microscope. Data were analyzed by two-way ANOVA, with $p < 0.05$ considered significant. CI in mice impacted motor skills, balance, coordination, and social behavior, with subsequent modulation by environmental factors observed longitudinally. The findings underscore the importance of intervention type for post-CI motor recovery. It is demonstrated that motor and cognitive functions, which are related to sociality, are enhanced by physical enrichment and environmental enrichment. However, social enrichment with healthy mice did not provide the same benefits and was linked to continued motor problems. Additionally, overexpression of BOD1, which plays a key role in motor function, was observed in specific groups. This study uniquely highlights the effects of various enrichment types on motor and sociality-related cognitive processes post-CI and identifies BOD1 as a potential biomarker for effective therapeutic strategies.

Key words: Cerebellar Infarct, Enriched Environment, Motor Skills, Social Interaction

ÖZET

Ayten, K. (2024) Serebellar Enfarktılı Fare Modelinde Sosyal ve Fiziksel Zenginleştirilmiş Çevrenin Sensorimotor ve Sosyal Performans Üzerindeki Etkileri. Yeditepe Üniversitesi, Sağlık Bilimleri Enstitüsü, Fizyoloji Anabilim Dalı, Yüksek Lisans Tezi, İstanbul.

Serebellar enfarktüs, ataksi gibi ciddi motor defisitlere yol açarak bireylerin günlük yaşam aktiviteleri ve öz bakım becerilerinde zorluk yaşamalarına ve dolayısıyla yaşam kalitelerinde ciddi azalmaya neden olan nadir bir inme türüdür. Bu çalışmanın amacı, serebellar enfarktılı fare modelinde çeşitli zenginleştirilmiş çevresel koşulların motor ve sosyal performans üzerindeki etkilerini değerlendirmek ve terapötik bir yaklaşım olarak potansiyel sonuçlarını araştırmaktır. C57BL/6 cinsi 40 erkek fare, fiziksel zenginleştirilmiş, zenginleştirilmiş çevre, zenginleştirilmiş çevre + 3 sağlıklı fare, standart barınma koşulları ve sham olmak üzere 5 gruba ayrılmıştır. Serebellar enfarkt modeli, farelere N5-(1-iminoetil)-L-ornitin dihidroklorürün stereotaksik enjeksiyonu ile indüklenmiştir. İnme öncesi ve belirli günlerde inme sonrası motor ve sosyal performans, ızgara telinde yürüme, yürüme analizi ve üç odalı sosyallik ve sosyal yenilik testleri kullanılarak değerlendirilmiştir. Serebellumda etkilenen alan, Hematoksin & Eozin boyama ile tespit edilmiştir. Motor koordinasyon ile ilişkili bir faktör olan Bioretention Defective 1 (BOD1), immünohistokimya yöntemi kullanılarak konfokal mikroskop ile görüntülenmiştir. Veriler iki yönlü ANOVA yöntemi ile analiz edildi ve $p < 0.05$ anlamlı olarak değerlendirildi. Bulgular, serebellar enfarktüs sonrası motor fonksiyon geri kazanımında müdahale türünün önemini vurgulamaktadır. Fiziksel ve çevresel zenginleştirmenin, motor ve sosyallik ile ilişkili bilişsel fonksiyonları artırdığı bulunmuştur. Ancak, sağlıklı farelerle yapılan sosyal zenginleştirme aynı yararı sağlamamış ve devam eden motor problemler ile ilişkilendirilmiştir. Ayrıca, motor fonksiyonda kilit rol oynayan BOD1 ekspresyonunun belirli gruplarda arttığı gözlemlenmiştir. Bu çalışma, serebellar enfarktüs sonrası çeşitli zenginleştirme türlerinin motor ve sosyallik ile ilişkili bilişsel süreçler üzerindeki etkilerini göstermekte ve BOD1'i etkili terapötik stratejiler için potansiyel bir biyomarker olarak tanımlamaktadır.

Anahtar Kelimeler: Serebellar Enfarktüs, Zenginleştirilmiş Çevre, Motor Performans, Sosyal Etkileşim

INTRODUCTION and PURPOSE

Ischemic stroke results from the thrombotic or embolic occlusion of cerebral or cerebellar arteries. Cerebellar stroke comprises approximately 2% to 3% of all stroke cases, with around 20,000 new cases of cerebellar infarction (CI) reported annually in the United States (1; 2). CI manifests through non-specific symptoms such as dizziness, nausea and vomiting, unsteady gait, and headache (3). The symptoms of cerebellar damage vary depending on the lesion's location within the cerebellum. Damage to the anterior lobe predominantly causes motor symptoms such as balance disorders, ataxia, dysmetria, and dysarthria, whereas damage to the posterior lobe predominantly results in cognitive symptoms related to executive function, spatial cognition, and language processes (4). Furthermore, the mortality rate following CI is higher compared to the mortality rate associated with infarction in other parts of the brain (5).

CI rehabilitation aims to facilitate movement and promote increased functionality. Rehabilitation strategies may include the use of visual and verbal cues to improve walking speed and step length, the use of assistive technology to facilitate computer use, and the provision of customized seating to maintain posture, balance, and coordination (6). Additionally, electrotherapy modalities such as biofeedback are utilized to aid in recovery (7). The combined use of strengthening, balance, and coordination exercises has been supported by some studies to improve standing balance (8). However, research on the effectiveness of resistance training using weights for improving upper extremity function remains variable, with reports of both positive developments and impairments in function (9). Consequently, the existing therapy methods for these patient groups are insufficient, indicating the need to explore new treatment models.

Enriched Environment (EE) refers to the enhancement of an individual or animal's social or physical surroundings with diverse stimuli aimed at promoting overall well-being (10). It has the potential of being an effective therapeutic intervention for stroke rehabilitation in rodents and provides various sensory, motor, cognitive, and social stimulations compared to the standard environment (11). Some clinical studies support that increased activity levels in an EE positively affect motor function, mood, and quality of life in these patient groups in a cost-effective manner (12). However, some aspects related to the mechanisms of action of EE and its systematic effects on brain regions in healthy and

pathological animal models remain unclear (13). Additionally, in the literature, socialization within the scope of EE is defined as enabling direct or indirect interaction between pairs or groups of the same species within a specific housing area (14). However, in daily life, the social circles of disabled individuals mostly consist of healthy individuals. There are studies that define socialization as interactions that occur between disabled individuals and their healthy family members and friends (15). Based on this viewpoint, we suggested that interactions between experimental group mice and healthy mice will result in distinct outcomes. The aim of this study was to investigate the effects of different types of EE, which provided various social and physical opportunities, on a CI mice model. It was hypothesized that different types of EE could result in varying effects on motor and social performance in the CI mice model. Furthermore, we put forward that these research findings may offer valuable contributions to future clinical studies.

2. GENERAL INFORMATION

2.1. Cerebellum

2.1.1 Anatomy and Organization of the Cerebellum

In mammals, the cerebellum is located above the brainstem and behind the occipital lobe, and anatomically it is divided into several regions. The central part (vermis) develops from the corpus, while the outer part (flocculus) develops from the auricle and hemispheres. The vermis and hemispheres are continuous with each other, and according to some theories, the hemispheres are lateral extensions of the vermis (16).

The cerebellar cortex is anatomically divided along the anteroposterior and mediolateral axes. When examining the cerebellum along the anteroposterior axis, it is divided into lobes and lobules. The vermis region of mammals' cerebellum is segmented into 10 lobules by folial fissures. These lobules are grouped into three primary lobes: anterior lobe (I-V), posterior lobe (VI-IX), and flocculonodular lobe (X). The anterior lobe is also known as the spinocerebellum, the posterior lobe as the cerebrocerebellum, and the flocculonodular lobe as the vestibulocerebellum (17).

The cerebellar cortex of the vermis is divided into four horizontal regions: the anterior region (lobules I-V), the central region (lobules VI-VII), the posterior region (lobules VIII-IX), and the nodular region (lobules IX-X). These four regions are further divided into parasagittal stripes. A similar arrangement is observed in the hemispheres (Figure 1). Lobules II-III are called the central lobule, lobules IV-V are called the culmen, and lobule VI is referred to as the simple lobule. Lobule VII is divided into crus I and crus II in the lateral hemisphere (18).

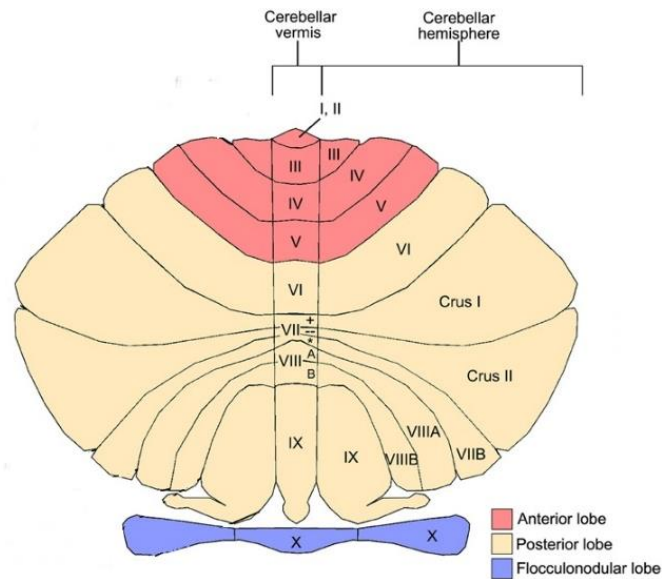


Figure 1. Schematic diagram of the lobes and lobules of the cerebellar cortex (19).

Although the cerebellar cortex is divided into sections, it does not have a structure as complex as that of the cerebral cortex. The entire cerebellar cortex consists of three cell layers. The outer layer, known as the molecular layer, contains the dendrites of Purkinje cells, the parallel-fiber axons of granule cells, and scattered inhibitory interneurons. The middle layer contains the cell bodies of the Purkinje cells. The inner layer, the granular layer, is densely packed with the cell bodies of granule cells and Golgi cells. Beneath these three layers is the white matter, which contains the afferent and efferent cerebellar axon.

2.1.2. Function and Functional Map of the Cerebellum

Afferent pathways reaching the cerebellum travel via the inferior and medial cerebellar peduncles. The largest of these pathways are mossy fibers, which have four main sources:

1. **The spinocerebellar pathway** involves the spinal cord and the external cuneate nucleus, sending ipsilateral and contralateral projections to the anterior lobe (lobules I-V) and lobule VIII of the vermis.
2. **The pontocerebellar pathway**, originating from the pontine nuclei, distributes throughout the cerebellum and particularly terminates in lobules VI-VIII of the vermis.

3. **The vestibulocerebellar pathway** features primary vestibular root fibers that terminate in the flocculonodular lobe and lobules IX-X of the vermis.
4. **The reticulocerebellar pathway** connects the lateral reticular nucleus connecting to the cerebellum via the inferior cerebellar peduncle, extending throughout the cerebellar cortex similarly to the spinocerebellar and vestibulocerebellar systems (16).

Mossy fibers terminate in cell-free synaptic glomeruli in the granular layer, forming glutamatergic synapses with granule cell dendrites, which then interact with Purkinje cell dendrites.

The second major afferent pathway, consisting of climbing fibers from the inferior olivary nucleus, crosses the base of the brainstem via the inferior cerebellar peduncle into the cerebellum. They ascend through the granular layer to synapse directly with Purkinje cell dendrites in the molecular layer. Notably, the olivocerebellar pathway has a parasagittal stripe organization, where each inferior olivary nucleus targets specific Purkinje cells, and each Purkinje cell is excited by a single climbing fiber (20). The olivocerebellar pathway is organized so that each inferior olivary nucleus stimulates specific parasagittal bands of Purkinje cells, and each Purkinje cell is excited by only one climbing fiber (21).

The cerebellum's fundamental cycle involves climbing and mossy fibers, which excite the cerebellar nuclei. This excitation is strongly inhibited by descending Purkinje cell axons from the cerebellar cortex. Additionally, cerebellar and vestibular nuclei regulate these fibers by sending inhibitory signals through Purkinje cell axons (16).

Neuroimaging studies in humans have validated somatotopic representations in the cerebellum (Figure 2) (22). The cerebellar functional map shows regions functionally connected to specific cerebral networks, with inverted topography evident in the contralateral cerebellum from foot, hand, and tongue representation areas (23). Using task-based functional magnetic resonance imaging (fMRI), researchers had subjects execute movements that illustrated maps of both gross motor topography (foot, hand, tongue, and lips) and fine motor topography (elbow, wrist, and multiple individuated finger movements). The representation was identified, extending from lobule IV-V of the anterior lobe, which includes regions responsible for the foot, arm, and fingers. This configuration continues just beyond the primary fissure in lobule VI, encompassing areas associated with the tongue and lips (24).

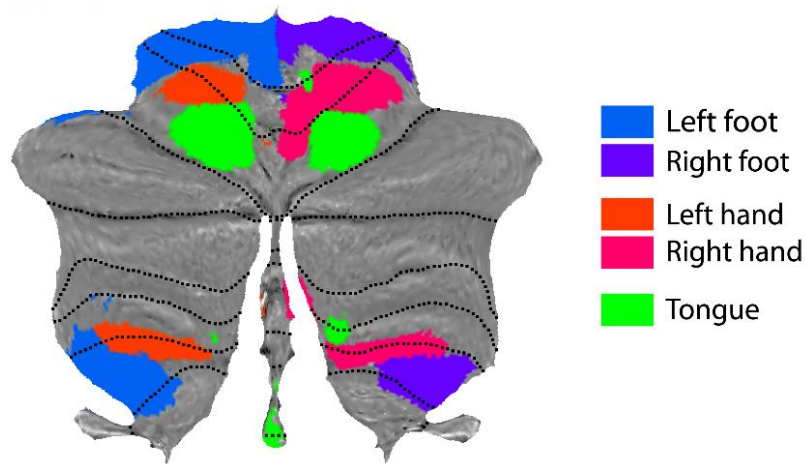


Figure 2. Somatotopic representations of cerebellum (22).

The lobes of the cerebellum play critical roles in various motor, sensory, and cognitive functions:

Lobules I-V: Associated with the spinocerebellar pathway. Ensure precise coordination of arm and leg movements (16).

Lobules II-III: Critical for the coordination of reflexive and voluntary movements of the hindlimbs.

Lobules IV-V: The structure associated with the forelimbs, as demonstrated in Figure 2, which is essential for the coordination of reflexive and voluntary movements, has been identified (22). Additionally, recent researches have suggested that lobules IV/V of the anterior lobe are involved in non-motor functions, such as social behavior, temporal memory (25), and working memory (26; 27).

Lobule VI: Coordinates facial muscle movements. Integrates sensory and motor functions. Aids in head and neck coordination (28).

Lobules VI-VII: Integrated with the pontocerebellar pathway. Crucial for planning, initiating, and timing complex motor movements. Process visual and auditory stimuli for broad sensorimotor integration. Involved in cognitive and limbic functions according to recent studies (29). Lobule VII is connected to circuits responsible for threat detection, behavioral flexibility, arousal, sensory-motor integration, and cardiorespiratory functions. This suggests that lobule VII might be involved in an anxiety module due to extensive connections between the cerebellum and anxiety-related brain areas (30).

Lobe X: Receives direct input from the vestibular system. Vital for balance and posture control (16).

Crus I and II: Involved in cognitive functions, especially working and spatial memory. Have significant associations with the hippocampus, highlighting their role in learning processes (31). Furthermore, the functions of the Crus I and Crus II regions include the assessment of social interactions and the regulation of emotional responses. Damage to these regions has been found to result in difficulties in social communication, a lack of empathy, and problems in understanding social cues (32).

In addition to its critical roles in motor functions, the cerebellum is also considered to play an essential role in supporting social behaviors and social learning processes. This is significant for understanding the cerebellum's complex relationships with cognitive functions and its impact on information processing networks within the brain (Figure 3) (33).

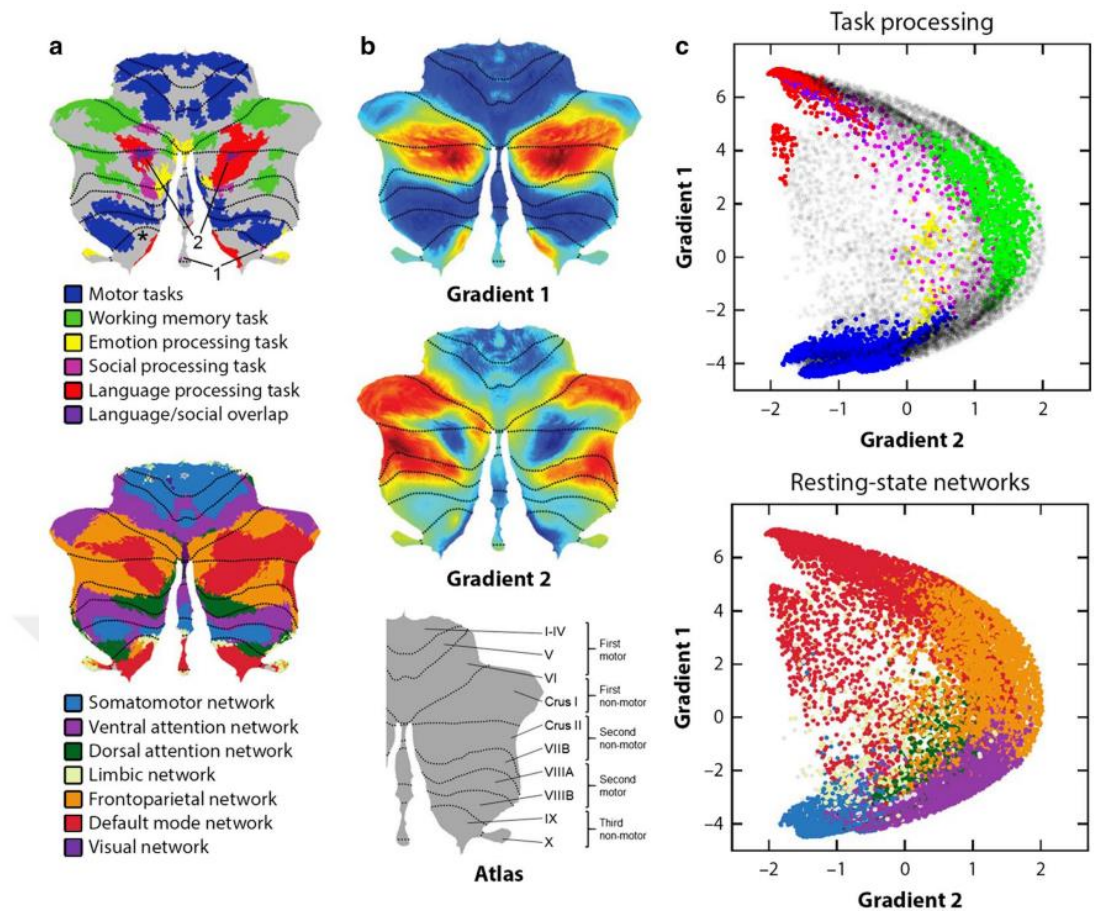


Figure 3. **a** Cerebellar task activation maps and resting-state networks. **b** Cerebellar functional gradients. **c** Relationship of functional gradients 1 and 2 with task activation maps and resting-state networks (34).

2.2. Cerebellar Infarct

2.2.1 Pathophysiology

The cerebellum is supplied by three primary arteries: the posterior inferior cerebellar artery (PICA) for the posterior surface, the anterior inferior cerebellar artery (AICA) for the inner auditory canal, and the superior cerebellar artery (SCA) for the upper and anterior surfaces (35). Studies indicate that CI more frequently affect the SCA supply region (36).

Occlusion of any of the three arteries supplying the cerebellum results in infarcts larger than 1.5 cm, often associated with cardioembolic or arteriosclerotic causes. Magnetic resonance imaging (MRI) studies have shown that microinfarcts, smaller than 1.5 cm, are

more common. These microinfarcts are typically located in the cerebellar cortex and the distal cortical areas of large arteries (37).

The clinical symptoms of CI vary depending on the affected region. Infarcts in the anterior lobe primarily cause motor issues (balance problems, ataxia, dysmetria, dysarthria), whereas infarcts in the posterior lobe result in cognitive and emotional disturbances (executive dysfunction, emotional instability) (38).

2.2.2. Epidemiology and Clinical Findings

According to the database, in 2019, the global mortality attributed to stroke reached a total of 6,552,725 deaths (39). Over the past 30 years, 80% of developing countries have experienced a transition in disease patterns from communicable to noncommunicable diseases. Among these, stroke stands out as one of the most common disabling conditions and the second leading cause of death (40; 41; 42). Ischemic strokes are the most prevalent type of cerebrovascular event, constituting approximately 55-90% of all stroke cases (43; 44). Within this extensive category, cerebellar infarction (CI) is considered relatively uncommon, accounting for about 2-3% of all ischemic stroke occurrences (45). This highlights the need for specialized awareness and diagnostic consideration for CI given its distinctive clinical manifestation and implications. In the United States, approximately 20,000 cases of cerebellar stroke are reported annually. Among these, infarctions involving the PICA occur more frequently than those involving the SCA, while AICA infarcts are relatively rare. The clinical presentation of CI typically includes symptoms such as dizziness, imbalance, nausea, vomiting, nystagmus, and ipsilateral occipital headache (46; 47). Coordination problems affect approximately 60-70% of patients (46; 48).

AICA occlusion presents a distinct set of symptoms. These symptoms include vertigo, ataxia, dysarthria, tinnitus, ipsilateral facial paralysis, hearing loss, trigeminal sensory loss, and Horner's syndrome. Furthermore, if the lateral pons is affected, contralateral sensory loss or hemiparesis may also occur. This clinical presentation offers crucial insights for both diagnosis and treatment (49).

CI often results in social isolation, significantly affecting an individual's overall well-being. The resultant deficits in balance, coordination (50), and speech can make social interactions challenging and frustrating for both the affected individuals and their social networks (51). These physical impairments, coupled with potential emotional and

cognitive difficulties, can lead to withdrawal from social activities and decreased participation in community life. This isolation is further aggravated by feelings of embarrassment and low self-esteem, which discourage individuals from seeking social engagement (52). Consequently, the lack of social interaction not only worsens mental health issues (53) such as depression and anxiety but also hinders rehabilitation and recovery. Addressing social isolation in patients with CI requires a multidisciplinary approach, involving medical treatment, physical rehabilitation, and social support systems to promote re-engagement and improve quality of life (54).

2.2.3. Prognosis

Infarcts affecting the PICA area are generally benign, although some patients may experience prolonged dizziness or walking imbalance (49). In severe cases, brainstem compression and cerebellar edema can lead to death. Partial PICA infarcts are milder, and symptoms typically resolve within weeks or months (55). Infarcts in the PICA area combined with AICA or SCA infarcts are more severe and commonly present with a pseudo-tumoral pattern (56).

In SCA infarcts, a pseudo-tumoral presentation has been observed in 21% of autopsy cases and led to coma and death in 7% of cases (57; 49). Most SCA infarcts have a benign prognosis.

AICA infarcts generally have a better prognosis without massive edema, but some cases may result in tetraplegia and coma. Surviving patients often exhibit peripheral facial palsy, trigeminal sensory symptoms, or hearing loss (47).

2.2.4. Treatment

The treatment of CI involves a multidisciplinary approach that includes emergency medical intervention such as thrombolytic therapy, surgical intervention, medication therapy such as antiplatelet drugs, lifestyle changes like incorporating a healthy diet and regular exercise routine, and rehabilitation such as physical therapy for functional recovery (58).

Existing CI rehabilitation aims to facilitate movement and promote increased functionality. Strategies may include the use of visual and verbal cues to improve walking speed and step length, the use of assistive technology to facilitate computer use, and customized seating areas to maintain posture, balance, and coordination (59). Electrotherapy modalities such as biofeedback are also utilized in rehabilitation for

recovery (60). The combined use of strengthening, balance, and coordination exercises has been supported by studies to improve standing balance (61). Research on the effectiveness of resistance training to improve upper extremity function has shown variable results. While resistance training may be beneficial in supporting the recovery of stroke patients, the current evidence is insufficient for evidence-based rehabilitation (62). Consequently, the existing therapy methods for these patient groups are insufficient for their full recovery and return to their previous daily routines, emphasizing the need for exploring new treatment models.

2.3 Enriched Environment

Enriched Environment (EE) refers to an environment that is designed to provide sensory and intellectual stimulation that can significantly promote cognitive, social, and physical development (63). This concept has been widely studied in both animals and humans. Research has demonstrated that EE can lead to numerous positive outcomes, such as increased brain plasticity, enhanced learning abilities, improved mental health, and even physical health benefits (64). In animals, EE has been associated with increased neuronal growth and connections in the brain (65; 66). In humans, exposure to EE has been linked to better cognitive function and resilience to stress and age-related decline.

This intervention has shown to be effective in infarct rehabilitation, particularly in rodent models, where it provides various sensory, motor, cognitive, and social stimulations compared to the standard environment. (67). An EE typically includes a variety of objects, increased physical activity opportunities, and enhanced social interactions, all of which contribute to neuroplasticity and functional recovery. By introducing complex physical surroundings, social interactions, and novel experiences, enriched EE engages and challenges the brain, fostering overall development and well-being (68).

Several clinical studies have also indicated that increased activity levels in an EE can positively impact function, mood, and quality of life in infarct patients cost-effectively. Patients exposed to EE often shows greater improvements in rehabilitation outcomes due to the comprehensive and stimulating nature of their surroundings (69).

Despite the promising results, some aspects related to the mechanisms of action of EE and its systematic effects on various brain regions in both healthy and pathological animal models remain unclear. Specifically, the precise biological processes through which EE enhances neural plasticity and cognitive function are not fully understood (25; 69). This

includes understanding which specific elements of the EE (such as social interaction or physical activity) are the most critical contributors to these benefits. These gaps highlight the need for further research to fully understand how enriched EE can be optimized for therapeutic use.

In addition to the physical and cognitive benefits, socialization is a critical component of EE. Socialization within the scope of EE is defined as enabling direct or indirect interaction between pairs or groups of the same species within a specific housing area (70). However, this concept needs to be adapted when considering human applications. In daily life, the social circles of disabled individuals predominantly consist of healthy individuals, rather than other disabled individuals. Therefore, socialization should also include interactions between disabled individuals and their healthy family members and friends, which can provide emotional support and enhance the overall rehabilitation process.

Some studies have started to explore socialization in this broader context, defining it as interactions between disabled individuals and their healthy family members and friends (71). These interactions not only support the rehabilitation process but also help integrate disabled individuals more fully into their community and social circles, promoting better mental health and well-being (70). Overall, EE offers a holistic approach to rehabilitation, addressing multiple facets of recovery and providing a comprehensive framework for improving outcomes in infarction and other neurorehabilitation contexts.

2.4 Biorientation Defective 1

Biorientation Defective 1 (BOD1) is primarily recognized for its critical role in chromosome alignment and segregation during cell division. This protein ensures that chromosomes are properly oriented and divided, which is essential for the accuracy and fidelity of cell division (25). Dysregulation or mutations in BOD1 can lead to chromosome misallocation and chromosome number abnormalities which are associated with cancer and other genetic disorders (72).

In a recent study, the neural circuitry between lobules IV/V of the cerebellar vermis and the fastigial nucleus (FN) was investigated, focusing on its role in sensorimotor coordination. BOD1 was identified as a key molecular component in this circuit, where deficits in Purkinje cells in lobules IV/V lead to hyperactivation of CaMKII α ⁺-neurons in the FN, resulting in ataxic behavioral symptoms (73). Remarkably, restoring BOD1

expression in the Purkinje cells of lobules IV/V was shown to reduce the ataxic symptoms in mice with a BOD1 deficiency driven by L7-Cre; BOD1^{fl/fl} genotype, highlighting the therapeutic potential of BOD1 modulation in cerebellar dysfunction (74).

In summary, new insights into the pathological mechanisms underlying cerebellar ataxia highlight the importance of the BOD1 protein in regulating the excitability of CaMKII α + neurons in the deep cerebellar nuclei. Recent reports suggest that dysregulation of BOD1 may contribute to the development of ataxia (Figure 4), and that targeting BOD1 or its downstream signaling pathways may have therapeutic potential for treating this condition (75).

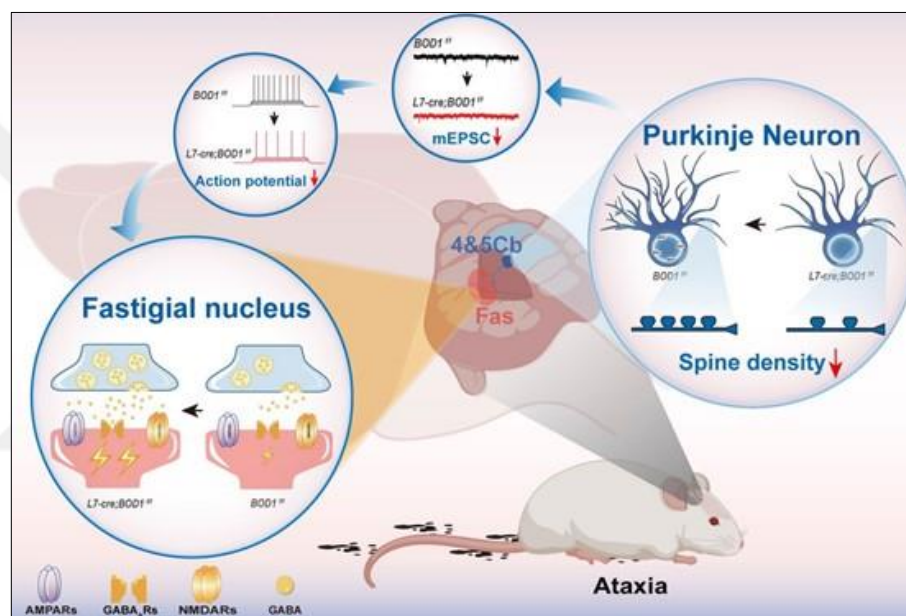


Figure 4. Schematic illustration how BOD1 regulates the cerebellar IV/V lobe Purkinje cells and their interaction with the FNCaMKII α + circuit that is associated with motor coordination (75).

The objective of this study was to investigate the effects of various forms of EE, which offer diverse social and physical affordances, on motor and social performance in a CI mouse model. Additionally, the study aims to examine changes in the BOD1 factor, which plays a key role in ataxia-related mechanisms, under different EE exposures in the targeted region.

3. MATERIALS AND METHODS

3.1. Experimental Animals

Forty male C57BL/6J mice aged 9-10 weeks were randomly assigned to groups. The mice were fed ad libitum and housed under appropriate light-dark cycles (12 hours light / 12 hours dark cycle) at a temperature of 22 ± 1 °C. The study was based on the induction of CI followed by the application of various EE interventions. The research protocols received approval from the Yeditepe University Local Ethics Committee.

3.2. Mouse Production Strategy

The mice used in the study were provided by the Yeditepe University Experimental Research Center in accordance with the experimental protocol.

3.3. Experimental Groups

Ensuring that each group consists of 8 mice, the animals were assigned to five different groups (Figure 5): physical enrichment (PE), enriched environment (EE), enriched environment with 3 additional healthy mice (EE+3), standard cage (STD), and sham.

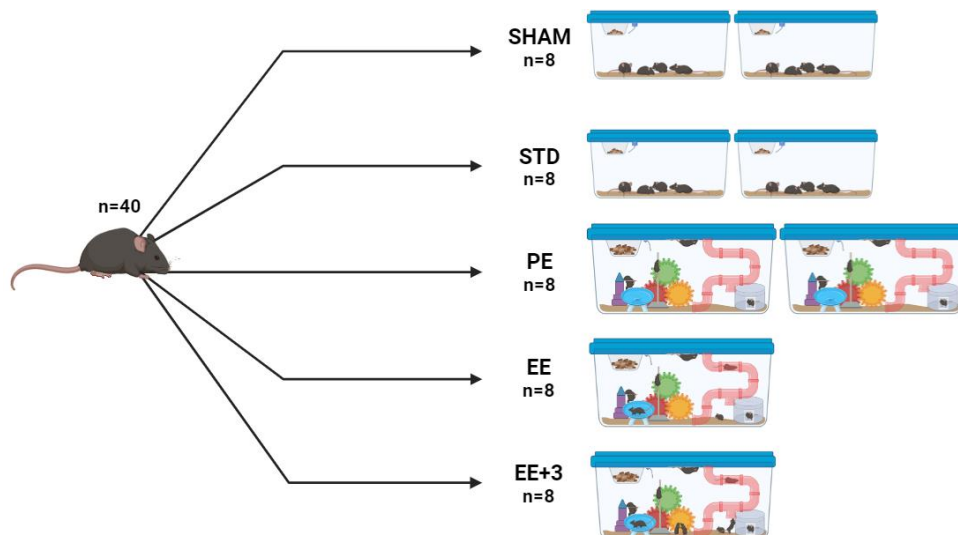


Figure 5. Experimental design and groups.

3.3.1 Sham Group

In the sham group, the CI model was not induced. Instead, physiological saline solution was injected via stereotaxis to simulate the procedure without creating the actual injury (Figure 6). Following the injection, no further intervention was performed to ensure that any observed effects could be attributed solely to the stereotaxic procedure, and not to subsequent treatments or manipulations.

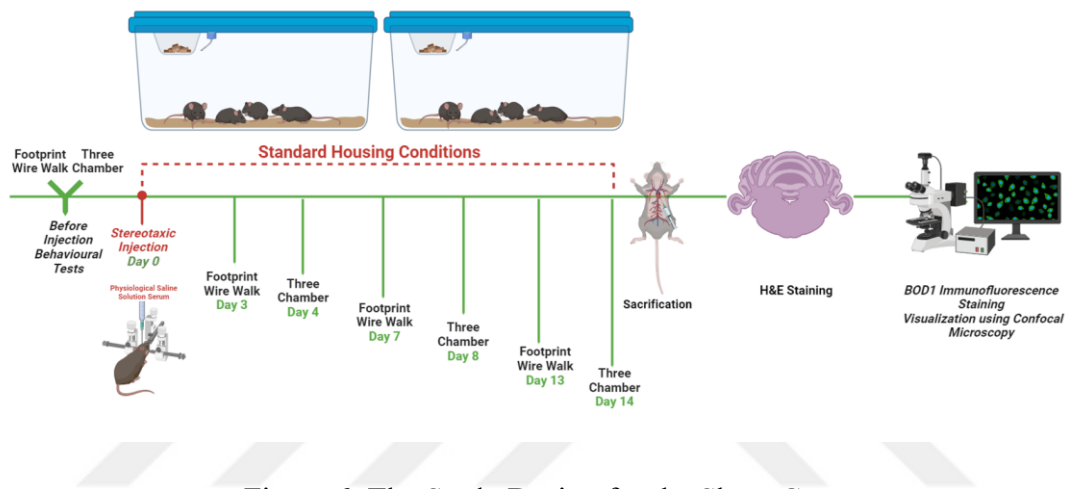


Figure 6. The Study Design for the Sham Group.

3.3.2. Standard Environmental Condition (STD) Group

In this group, the CI model was induced in mice via stereotaxic injection of N5-(1-iminoethyl)-L-ornithine dihydrochloride (Figure 7). After the injection, the mice were exposed in standard housing conditions, with no further interventions applied. This group was established to observe the natural progression and prognosis of CI without any intervention. The sensorimotor and social performances of the mice were regularly monitored. This setup serves as a control group to better isolate the effects of the CI model during experimental comparisons, allowing a clearer assessment of experimental interventions.

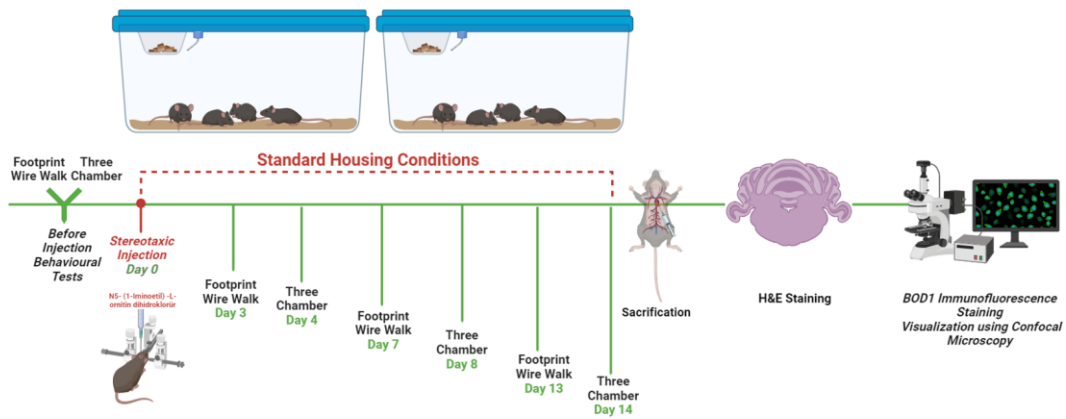


Figure 7. The Study Design for the STD group.

3.3.3. Physical Enrichment (PE) Group

In this group, the CI model was induced in mice via stereotaxic injection of N5-(1-iminoethyl)-L-ornithine dihydrochloride (Figure 8). After the injection, the mice were placed in cages with physical enrichment (PE). 8 mice were housed, with 4 mice per cage. These cages were larger than standard mouse cages and contained various objects such as boxes, wheels, chains, pipes, and ladders. The objects and their locations within the cage were changed at certain time intervals to create novelty. This setup was created to determine the effects of PE on the CI model during experimental comparisons.

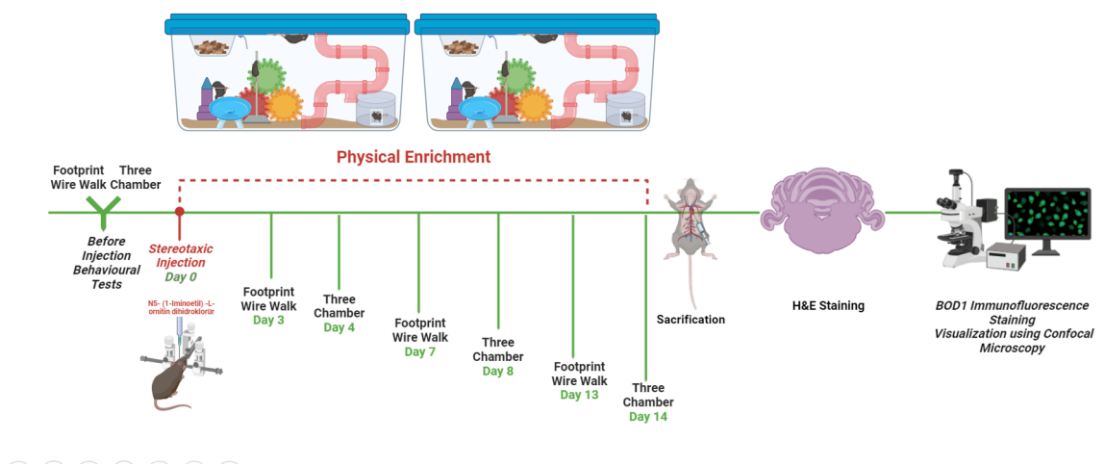


Figure 8. The Study Design for the PE group.

3.3.3. Enriched Enrichment (EE) Group

In this group, the CI model was induced in mice via stereotaxic injection of N5-(1-iminoethyl)-L-ornithine dihydrochloride (Figure 9). After the injection, the mice were placed in cages that included both physical and social enrichment. The physically enriched setting was adjusted in the same manner as in the PE group. For social enrichment, all CI mice were housed together in the same cage. This arrangement was designed to investigate the effects of social enrichment with CI mice on the CI mouse model.

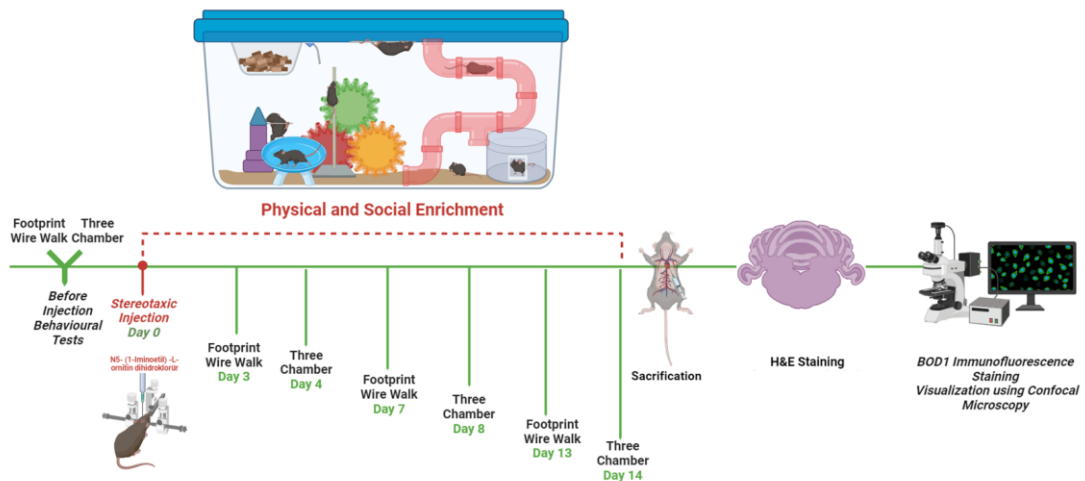


Figure 9. The Study Design for the EE group.

3.3.5. Enriched Enrichment+3 Healthy Mice (EE+3) Group

In this group, the CI model was induced in mice via stereotaxic injection of N5-(1-iminoethyl)-L-ornithine dihydrochloride (Figure 10). After the injection, the mice were placed in cages that included both physical and social enrichment. The physically enriched setting was adjusted in the same manner as in the PE group. For social enrichment, all CI mice were housed together in the same cage, and 3 healthy mice that had not undergone the CI procedure were added. This arrangement was designed to investigate the effects of social enrichment with healthy mice on the CI mouse model.

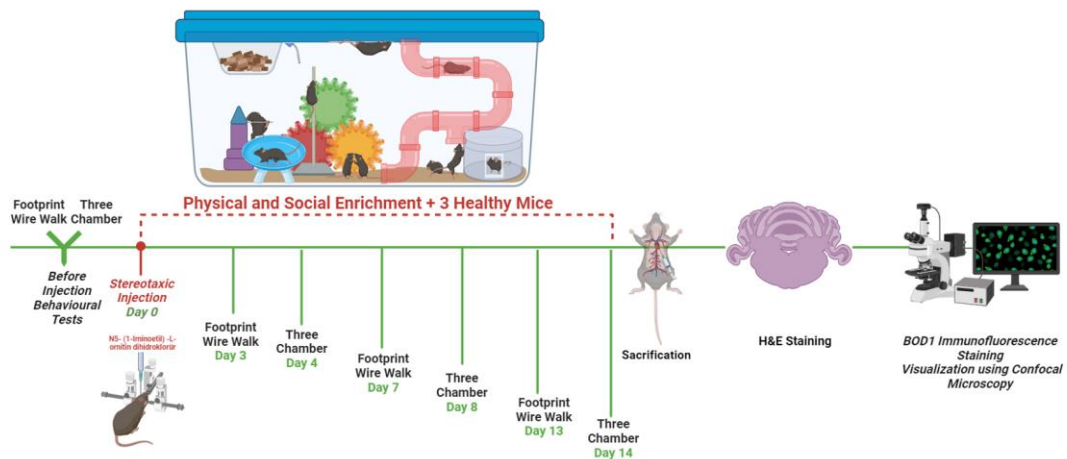


Figure 10. The Study Design for the EE+3 group.

3.4. Cerebellar Infarction Modelling

Under isoflurane anesthesia, the skin and subcutaneous tissue of the mice were incised to access the occipital bone. To induce a CI, a hole was drilled into the occipital bone using a micro-drill, just large enough for a needle to pass through.

To induce an infarction in the blood supply region of the SCA, the IV and V lobules of the cerebellum were targeted. A vasoconstrictor agent, N5-(1-Iminoethyl)-L-ornithine dihydrochloride (100 mM, Tocris), was injected using a Hamilton microinjector at a perpendicular angle into the cerebellum via a lateromedial route. This procedure aimed to induce vasoconstriction and focal ischemia at the injection site.

The injection of N5-(1-Iminoethyl)-L-ornithine dihydrochloride was administered at a volume of 2.4 μL and a rate of 0.1 μL per minute (Figure 11). The coordinates for the injection, relative to the bregma, were: antero-posterior -5.75 mm, medio-lateral -0.6 mm (right), and dorsa-ventral -0.9 mm. The micropipette was left to diffuse for 7 minutes to ensure proper distribution of the substance.

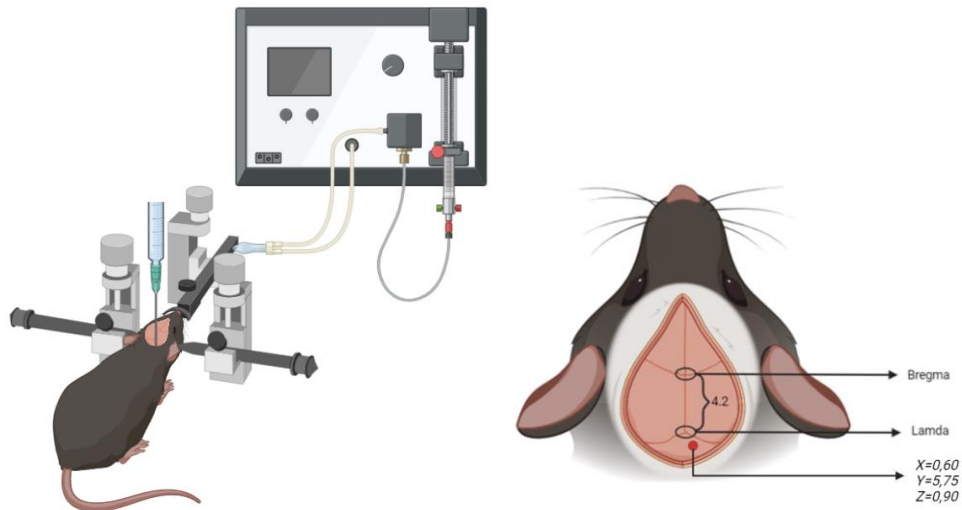


Figure 11. Stereotaxic Operation and Coordinates

In the sham group, the same procedure was performed, but instead of N5-(1-Iminoethyl)-L-ornithine dihydrochloride, physiological saline was injected intracranially (76).

3.5. Sensorimotor and Social Performance Assessment

Sensorimotor and social performance were assessed pre-infarct and on specific days post-infarct using the wire walk test, footprint test, and three-chamber test.

3.5.1. Footprint Test

The footprint test is a method used to examine the motor skills and walking patterns of mice. The gait analysis protocol and analysis were performed according to the Brooks 2012 protocol (77).

Materials

- 70% ethanol alcohol
- Two A4 white papers
- 60 cm long, 5 cm wide corridor with high walls
- Dark box for the mouse to escape at the end of the walk
- Two different non-toxic water-based paints
- Cup for pouring the paints

Test Procedure

Thirty minutes before the test, the mice were brought to the testing room for adaptation. After adaptation, the mice walked three times from the beginning of the corridor to the dark box. Then, the front paws were dipped in one container of paint (red paint), and the hind paws were dipped in the other container of paint (blue paint). The mice were allowed to walk from the beginning of the corridor to the dark box without running or stopping. After each test, the materials used were cleaned with 70% ethanol alcohol and allowed to dry.

Analysis

The times when the mice ran or stopped were marked and excluded from the analysis. Then, the steps on the paper were analyzed using a ruler. The analysis was conducted bilaterally, addressing both the right and left sides.

Step Length: It is the distance between the centers of the bases of the hind paws on the same side during the same step (Figure 12).

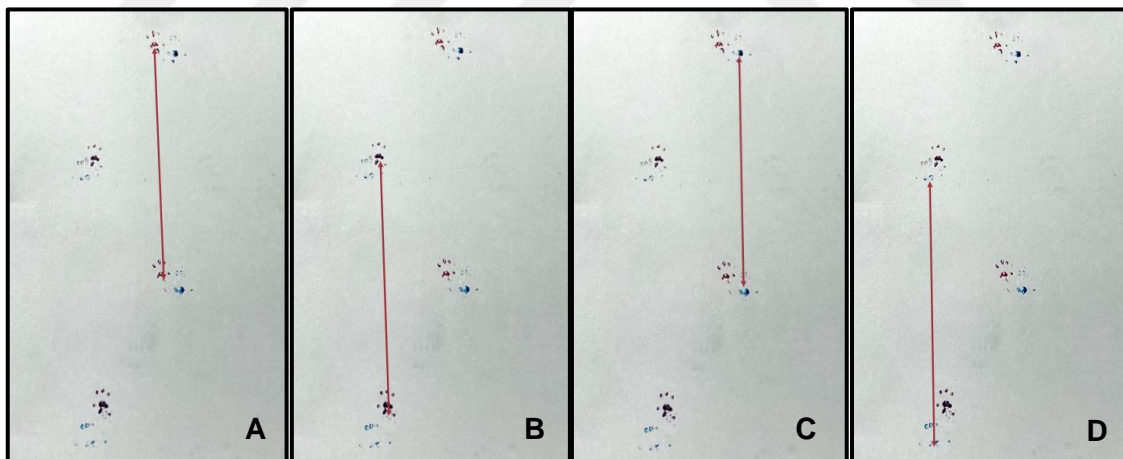


Figure 12. Footprint Sheet. The red arrows represent the step lengths, with **A** showing the right front, **B** indicating the left front, **C** illustrating the right hind, and **D** demonstrating the left hind.

Step Width: It is the measurement of the lateral distance between the front or hind paws. This variable has been assessed in two ways, with reference to both the right and left sides (Figure 13).

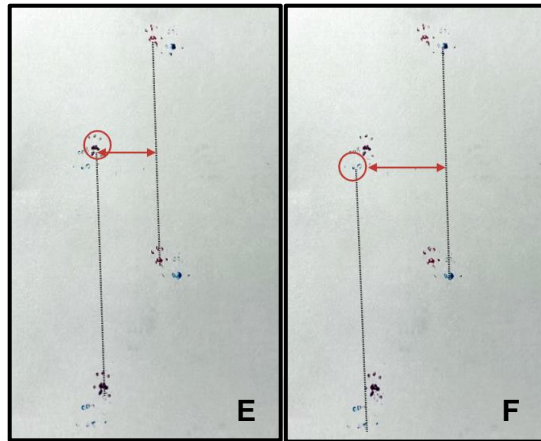


Figure 13. Footprint Sheet. The red arrows represent the step width. **E** represents the step width of the front paws, while **F** represents the step width of the hind paws.

Step Overlap Distance: It is the distance between the center of the base of the front paw and the center of the base of the hind paw on the same side (Figure 14). In an optimal gait cycle, the hind paw should precisely correspond to the position where the front paw initially made contact.

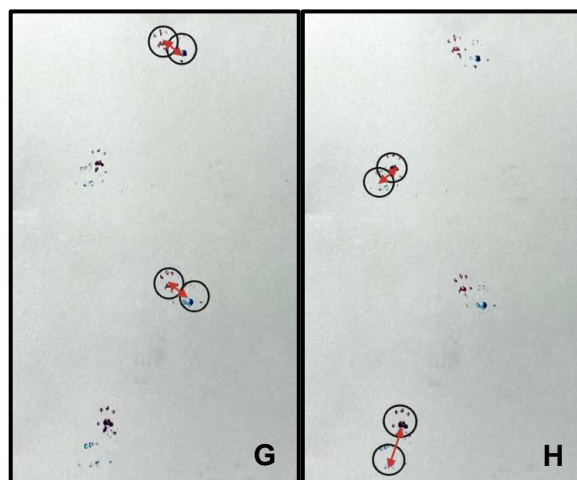


Figure 14. Footprint Sheet. The red arrows indicate the step overlap distance. **G** represents the right side, while **H** represents the left side.

3.5.2. Wire Walk Test

The wire walk test involves walking on a wire mesh grid and has been demonstrated to be effective in detecting motor deficits and motor coordination impairments (78). It has also proven to be effective in assessing the progress of post-stroke rehabilitation (79).

Materials

- Elevated wire grid
- Dark room
- Video camera
- 70% ethanol alcohol

Test Procedure

Thirty minutes before the test, the mice were brought to the testing room for adaptation. After an adaptation period, the mice will be placed on the wire grid and allowed to walk freely for 5 minutes (Figure 15 also see Figure 16). Following each test, the materials used will be cleaned with 70% ethanol alcohol and allowed to dry.

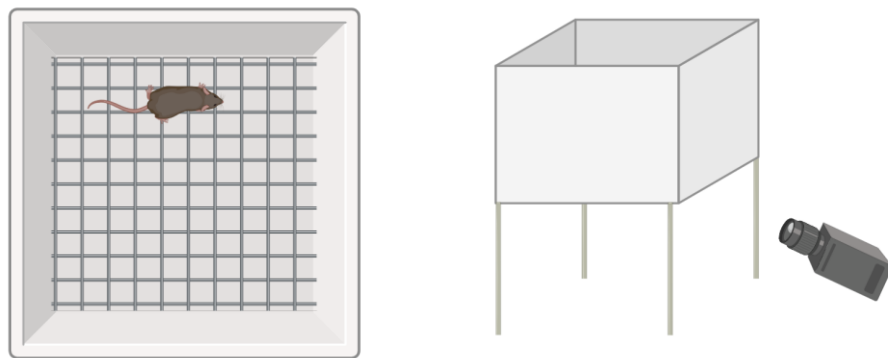


Figure 15. The Wire Walk Test Design

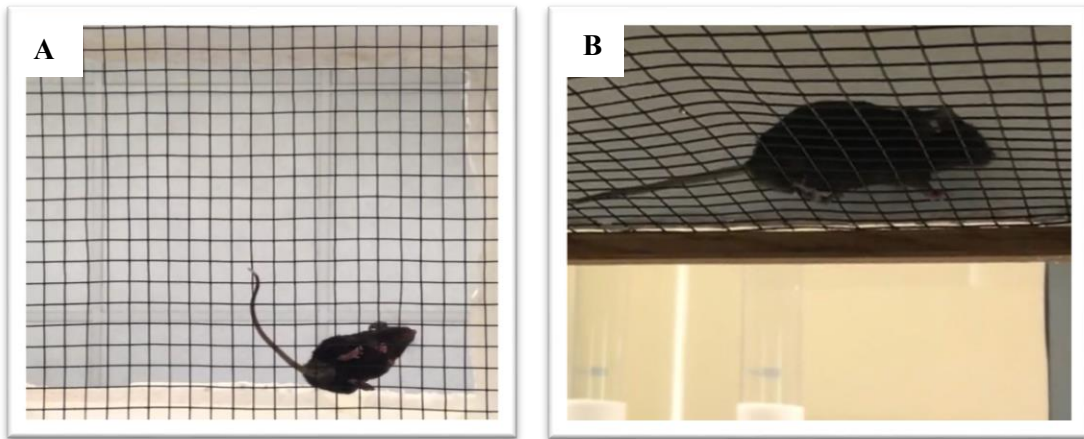


Figure 16. Moments from the video of the wire walk test: Picture **A** provides a bottom-up view, while Picture **B** offers a side view.

Analysis

The number of foot slips for each limb was recorded for every 100 steps observed through video analysis.

3.5.3. Three Chamber Test

The Three Chamber Test is a method used to assess social behaviors, particularly social interaction and social memory. This test is typically conducted on mice and consists of three stages. In the adaptation phase (Part 1), the tested animal is acclimated to the three-chamber test apparatus. Sociability (Part 2) is defined as the tendency to spend more time with another mouse rather than spending time alone in the same but empty chamber (Figure 17A). Social Novelty Preference (Part 3) is defined as the tendency to spend more time with an unfamiliar mouse compared to the time spent with an already-investigated mice (Figure 17B). The experimental design of the three-chamber test allows researchers to understand various dimensions of social behavior in mice, including their interest in new social opportunities and their memory of previous social encounters (80).

Materials

- Platform and Compartments: The Plexiglas platform (63x41x30 cm) is partitioned into three sections, each with small rectangular openings (5 cm wide x 3 cm tall).
- Side Compartments: Each side section consists of triangular areas where stranger mice are placed.

- The EthoVision video tracking system
- 70% ethanol alcohol

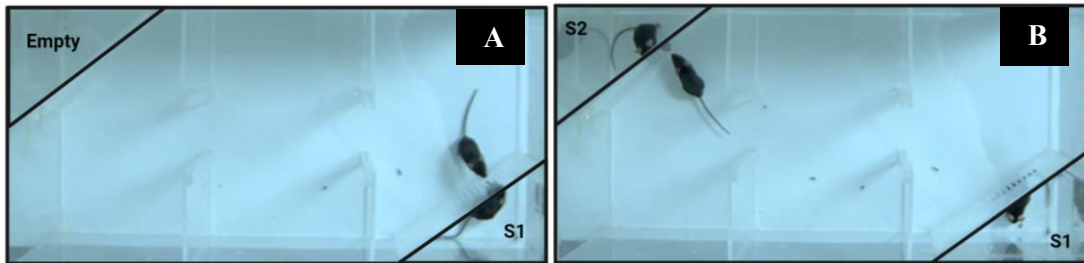


Figure 17. Three-Chamber Sociability and Social Novelty Preference Test. **A** sociability. **B** social novelty preference.

Test Procedure

This experiment consisted of three parts, each lasting for 10 minutes. In Part 1, the mice were placed in the three-chamber apparatus for 10 minutes to allow for free exploration and adaptation. In Part 2, a stranger mouse 1 (S1) was introduced into one chamber, and the frequency and duration of interactions between the experimental mice and S1 were recorded over the course of 10 minutes. In Part 3, another stranger mouse 2 (S2) was placed in the opposite chamber. During this part, the frequency and duration of interactions between the experimental mice and S2, in comparison to the previously encountered mouse, were recorded over 10 minutes. The EthoVision video tracking system was used to record the behaviors of the experimental mouse.

Analysis

The social preference index (SPI) was calculated using recorded cumulative duration data. SPI index is calculated using the following formula:

$$SPI = \frac{(\text{Spent Time in Social Chamber} - \text{Spent Time in Empty Chamber})}{(\text{Spent Time in Social Chamber} + \text{Spent Time in Empty Chamber})}$$

"Spent Time in Empty Chamber" refers to the duration of time a subject spends in a chamber that lacks any social stimulus or interaction. "Spent Time in Social Chamber" refers to the duration of time a subject spends in a chamber where a social stimulus (81).

This formula normalizes the measure of preference for the social chamber relative to the empty chamber by computing the difference between the two conditions and dividing by their sum. The resulting index ranges from -1 to 1. Specifically, an index value of 1 signifies a strong preference for the social chamber, a value of 0 indicates no noticeable preference, implying equal time spent in both chambers, and a value of -1 indicates a strong preference for the empty chamber. This normalized index allows for a standardized comparison of social preference across different subjects or experimental conditions.

The social novelty preference index (SNPI) is a quantitative measure used in behavioral studies to assess an individual's preference for a novel social environment compared to a familiar one. It is calculated using the formula:

$$SNPI = \frac{(Spent\ Time\ in\ Novelty\ Chamber - Spent\ Time\ in\ Social\ Chamber)}{(Spent\ Time\ in\ Novelty\ Chamber + Spent\ Time\ in\ Social\ Chamber)}$$

"Spent Time in Novelty Chamber " refers to the duration of time the subject spends in a chamber with a novel social stimulus. "Spent Time in Social Chamber" refers to the duration of time the subject spends in a chamber with a familiar social stimulus (81).

A value of 1 indicates a strong preference for the novelty chamber, while a value of 0 indicates no noticeable preference, implying equal time spent in both chambers. Conversely, a value of -1 indicates a strong preference for the familiar social chamber. This scale provides a clear and concise measure of social novelty preference, enabling researchers to assess and compare the inclination towards new social interactions versus familiar ones.

3.6. Cardiac Perfusion and Brain Slicing

Administer appropriate anesthesia to the subject to ensure pain-free procedure. After making a small incision in the right atrium, phosphate-buffered saline (PBS) was administered to the left ventricular circulation to remove the blood, followed by 4% paraformaldehyde (PFA) to fixate the brain tissue. To continue fixation, the extracted brain tissue was placed in a tube containing PFA solution. A vibrotome system was used to cross-section the brains at a thickness of 40-50 μm (Figure 18).

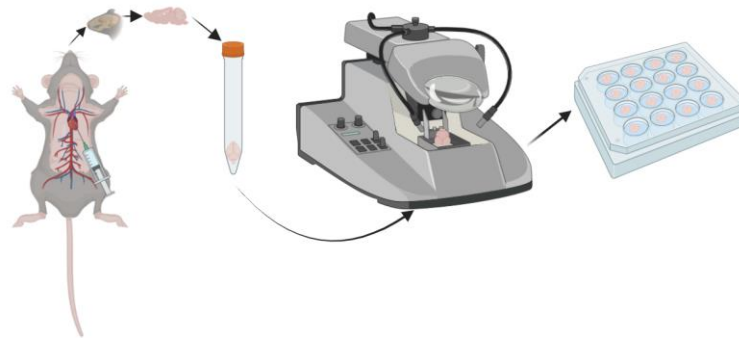


Figure 18. Schematic Representation of Cardiac Perfusion and Brain Slicing

3.7. Hematoxylin And Eosin Staining and Visualization

Hematoxylin and eosin (h&e) staining is a commonly used method that allows for detailed observation of cell and tissue anatomy. After the tissue was subjected to dehydration procedures, h&e staining was performed (Figure 19). After the staining process, the mounted slides were imaged using transmission electron microscopy (TEM) (Figure 20).

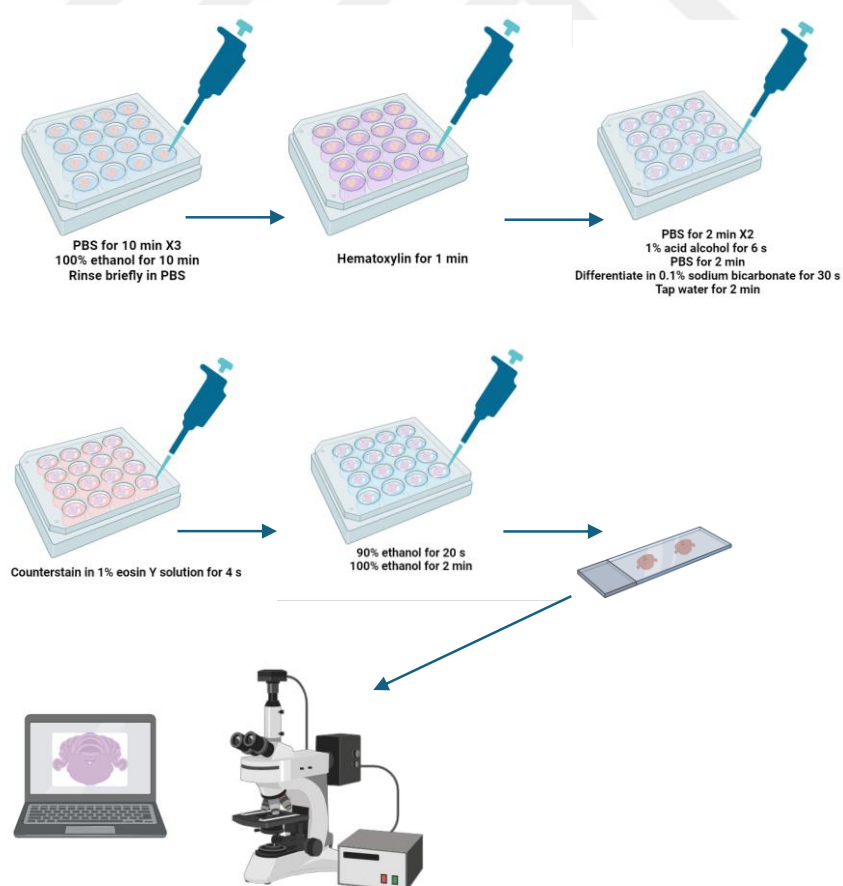


Figure 19. H&E staining procedure and visualization

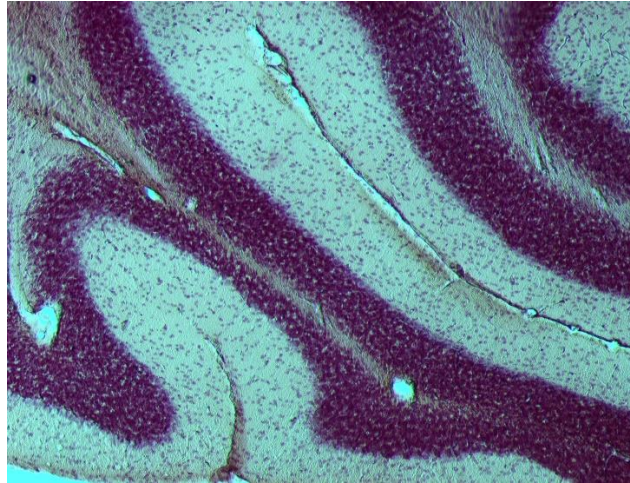


Figure 20. Image of cerebellum tissue post h&e staining captured at 20x magnification using TEM

3.8. Immunofluorescence Staining for Biorientation Defective 1

Following the immunofluorescence staining procedure (Figure 21) with specific primary antibodies on fixed tissue sections, the localization and expression of BOD1 were visualized using a confocal microscope. This method allowed for the precise examination of BOD1 distribution within the tissue, providing valuable insights into its spatial distribution in the cellular environment.

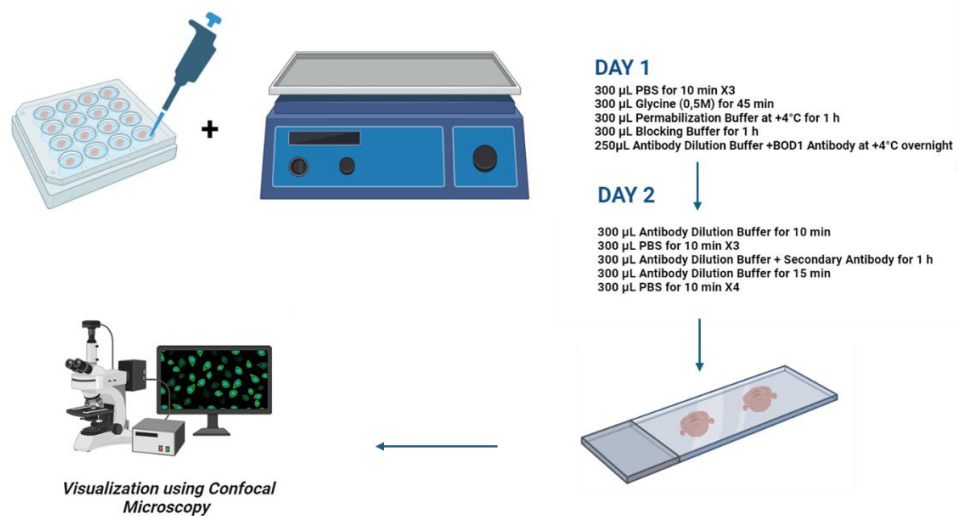


Figure 21. Immunofluorescence Staining procedure for BOD1

3.9. Statistical Analysis

The statistical analyses were performed using GraphPad Prism®8 software. Data were presented as number, percentage and mean \pm Standard Deviation (SD). The normal distribution of the data was assessed using the Shapiro-Wilk normality test. The comparison between groups was conducted using the two-way ANOVA method. A significance level of $P < 0.05$ was considered statistically meaningful. Figure illustrations were created using the BioRender program.



4. RESULTS

4.1. Sensorimotor and Social Performance Assessment Results

4.1.1 Footprint Analysis

The data analysis (Table 1), based on pre-injection metrics, was performed by applying percentage discrimination for each individual mouse.

4.1.1.1. Right Hind Step Length

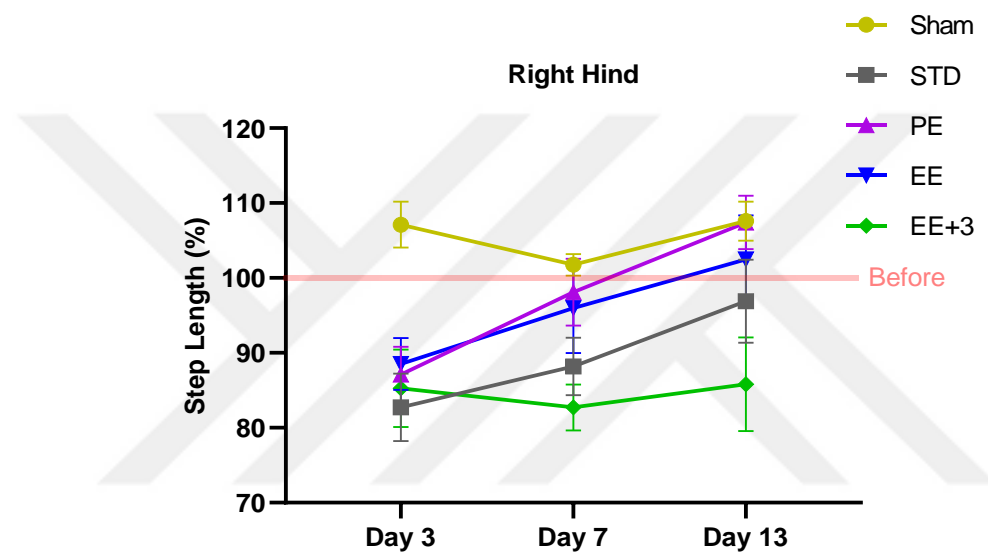


Figure 22. Right hind step lengths across experimental groups in the footprint test analysis. Two Way repeated measure ANOVA TUKEY's multiple comparison test, *** $p < 0,001$, ** $p < 0,01$, * $p < 0,05$

The statistical analyses revealed significant decreases on day 3 in right hind step lengths when comparing the sham group to the other groups: STD ($p = 0.0051$, **), PE ($p = 0.0076$, **), EE ($p = 0.0094$, **), and EE+3 ($p = 0.0251$, *).

When compared to baseline measurements, the right hind step length data for the SDT, PE, and EE groups showed a significant reduction on the 3rd day, with reductions observed in the SDT group ($p = 0.0254$), the PE group ($p = 0.0402$), and the EE group ($p = 0.0495$). In the EE+3 group, the variable showed a decreasing trend after the injection compared to baseline measurements, resulting in a statistically significant reduction on the 7th day ($p = 0.0033$ **). In the Sham group, no significant differences were found.

Following the 3rd day, the PE, EE, and STD groups showed an increasing trend in right hind step lengths. By the 13th day, the PE group demonstrated a statistically significant increase compared to the 3rd day ($p=0.0006$ ***).

On the 7th day, the STD group, which showed an increasing trend from the 3rd day, was compared with the sham group. The reduction in the variable decreased and the statistical significance observed on the 3rd day was lost ($p=0.0535$, not significant). The result remained close to the threshold for statistical significance.

In contrast, the EE+3 group exhibited a sustained and statistically significant decrease in right hind step lengths, which continued to decrease further from day 3 to day 7 (p -value = 0.0016, *), compared to the sham group. Furthermore, when compared to the baseline measurements, EE+3 group demonstrated a statistically significant decrease on the 7th day ($p=0.0033$, **).

No statistically significant differences were identified between the groups on day 13. However, the PE and EE groups reached above their baseline values, while the STD and EE+3 groups remained below their initial baseline values (Figure 22).

4.1.1.2. Left Hind Step Length

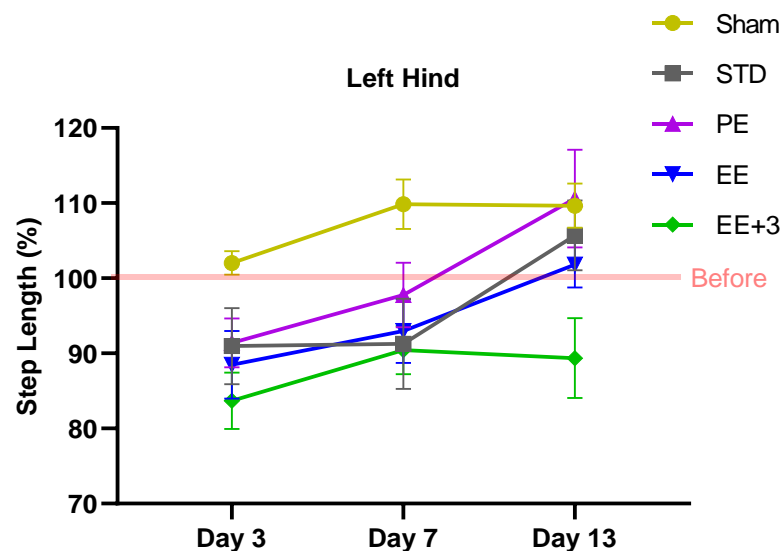


Figure 23. Left hind step lengths across experimental groups in the footprint test analysis. Two Way repeated measure ANOVA TUKEY's multiple comparison test, *** $p<0,001$, ** $p<0,01$, * $p<0,05$.

On day 3, the left hind step length data for the SDT, PE, and EE groups showed a decreasing trend compared to their baseline values and the sham group. In the EE+3 group, this decrease was statistically significant on day 3 both compared to the baseline values ($p=0,0137$, *) and the sham group ($p=0.0088$, **). In comparison to the Sham group, the EE+3 group exhibited a statistically significant decrease on day 7 ($P=0.0063$ **) and day 13 ($P=0.0427$ *).

The left hind step lengths of the PE and EE groups showed an increasing trend from day 3 to day 13. This increase was found to be statistically significant in the PE group when comparing the data from days 3 and 13 ($p=0,0046$, **).

All experimental groups surpassed their baseline values, except for the EE+3 group, which remained below its initial baseline values (Figure 23).

4.1.1.3. Right Front Step Length

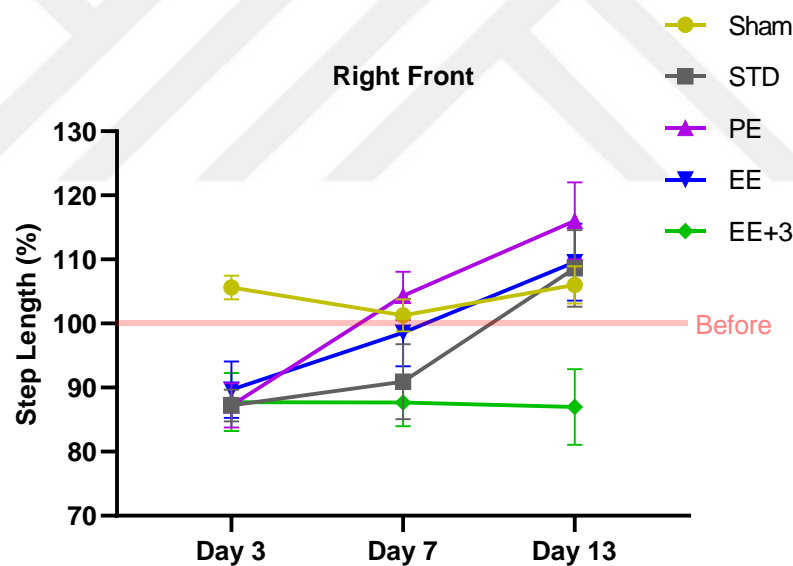


Figure 24. Right front step lengths across experimental groups in the footprint test analysis. Two Way repeated measure ANOVA TUKEY's multiple comparison test, *** $p<0,001$, ** $p<0,01$, * $p<0,05$.

The statistical analyses revealed significant decreases on day 3 in right front step lengths when comparing the sham group to the other groups: STD ($p=0,0004$, ***), PE ($p=0,0051$, **), EE ($p=0,0495$, *), and EE+3 ($p=0,0306$, *). Additionally, all groups, except for the sham group, exhibited a decreasing trend on day 3 when compared to their

baseline data. This decrease was statistically significant in the STD ($p=0.0053$, **) and PE ($p=0.0307$, *) groups.

On day 7, an increasing trend in this variable was observed in the SDT, PE, and EE groups. The increase in the PE group was determined to be statistically significant when compared to the day 3 data ($p=0.0362$, *). In contrast to the other groups, the EE+3 group exhibited a decreasing trend. This decrease was statistically significant on day 7 when compared to the baseline data ($p=0.0484$, *).

On day 7, a significant difference was observed between the PE and EE+3 groups ($p=0.0459$, *), which is a noteworthy finding. This statistically significant difference continued to increase on day 13 ($p=0.0271$, *).

In the comparison of the 3rd and 13th day data for the SDT and PE groups, the SDT group showed a statistically significant increase on the 13th day compared to the 3rd day ($p=0.0198$, *). Similarly, the PE group also exhibited a statistically significant increase on the 13th day compared to the 3rd day ($p=0.0004$, ***).

On day 13, all experimental groups exceeded their baseline values, except for the EE+3 group, which remained below its initial baseline values (Figure 24).

4.1.1.4. Left Front Step Length

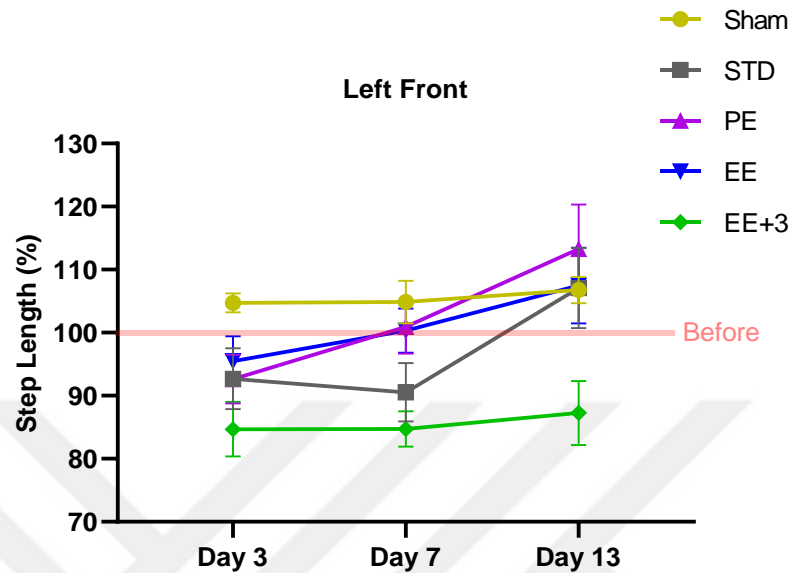


Figure 25. Left front step lengths across experimental groups in the footprint test analysis. Two Way repeated measure ANOVA TUKEY's multiple comparison test, *** $p < 0,001$, ** $p < 0,01$, * $p < 0,05$.

On the 3rd day, a decreasing trend in left front step length was observed in all groups except the sham group. This decrease is statistically significant in the EE+3 group when compared to the baseline data ($p=0.0370$, *) and when compared to the sham group ($p=0.0125$, *).

After the 3rd day, an upward trend was observed in both the PE and EE groups. Specifically, in the PE group, this increase reached statistical significance on the 13th day when compared to the 3rd day ($p=0.0227$, *).

On day 7, the EE+3 group showed a significant difference compared to the PE ($p=0.0500$, *), EE ($p=0.0265$, *), and Sham ($p=0.0034$, **) groups, indicating statistically noteworthy findings. Moreover, on the 13th day, the difference between the EE+3 group and the sham group continued to be statistically significant ($p=0.0365$, *). Additionally, when compared to the baseline data of the EE+3 group, the reduction continued after the 3rd day and maintained its significance on the 7th day with an increased reduction ($p=0.0041$, **).

On day 13, while the EE+3 group remained below its initial baseline, all other experimental groups exceeded their baseline values (Figure 25).

4.1.1.5. Hind Step Width

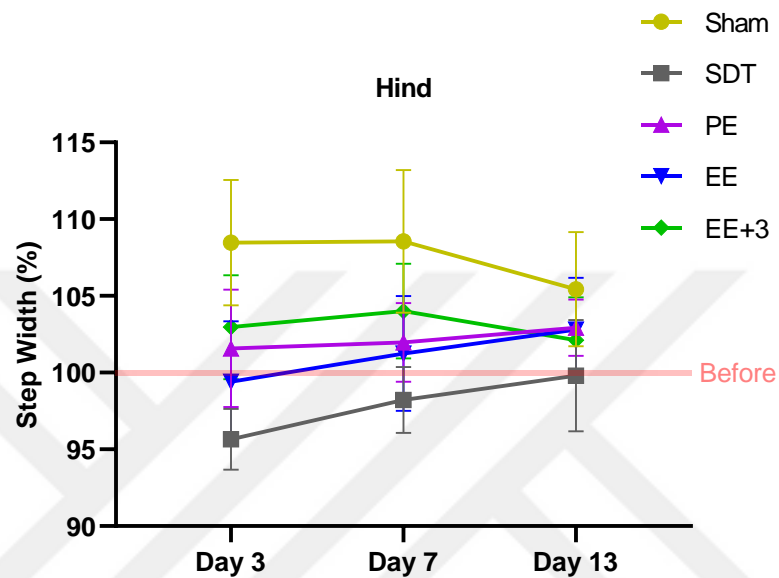


Figure 26. Hind step width across experimental groups in the footprint test analysis. Two Way repeated measure ANOVA TUKEY's multiple comparison test, *** $p < 0,001$, ** $p < 0,01$, * $p < 0,05$.

In the analysis of step widths in the hind limbs, no significant differences were found either between the groups or within the groups over time (Figure 26).

4.1.1.6. Front Step Width

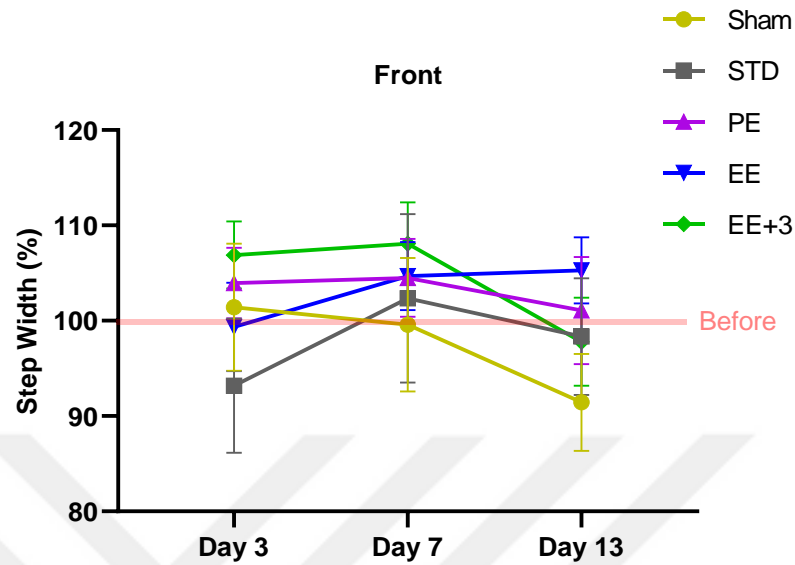


Figure 27. Front step width across experimental groups in the footprint test analysis. Two Way repeated measure ANOVA TUKEY's multiple comparison test, *** $p < 0,001$, ** $p < 0,01$, * $p < 0,05$.

In the analysis of step widths in the forelimbs, no significant differences were observed either between the experimental groups or within the groups over time (Figure 27).

4.1.1.7. Right Steps Overlap Distance

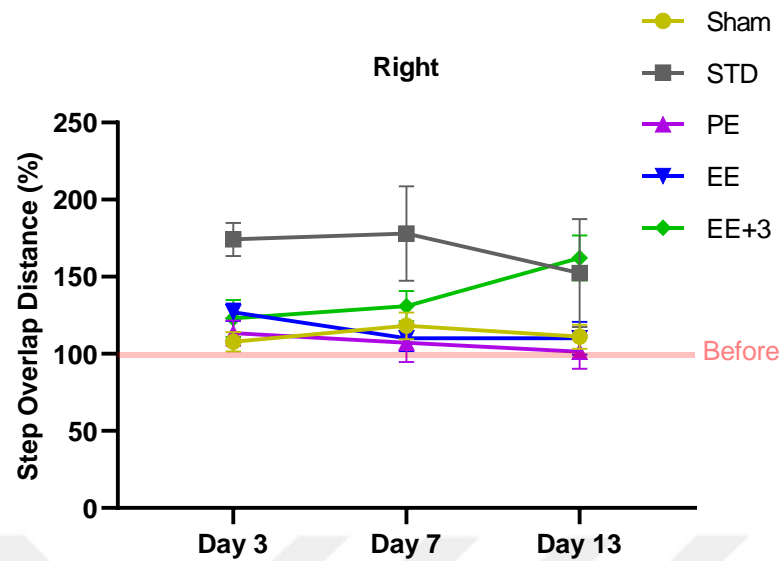


Figure 28. The right steps overlap distance across experimental groups in the footprint test analysis. Two Way repeated measure ANOVA TUKEY's multiple comparison test, *** $p < 0,001$, ** $p < 0,01$, * $p < 0,05$.

After the injection, on day 3, all experimental groups except for the Sham group showed an increasing trend in the right front overlap distance variable. This increase is statistically significant in the STD ($p=0.0010$, ***) and EE ($p=0.0080$, **) groups when compared to their baseline data. On the 13th day, this increasing trend reached statistical significance ($p=0.0149$, *) when compared to the baseline data in the EE+3 group.

The statistical analyses revealed a significant increase on day 3 in right step overlap distance when comparing the STD group to the other groups: Sham ($p=0.0016$, **), PE ($p=0.0042$, **), EE ($p=0.0175$, *), and EE+3 ($p=0.0446$, *).

On the 13th day, while this variable remained close to the baseline data in the PE group, an increase was observed in the EE+3 group. Notably, the comparison between these two groups demonstrated statistical significance ($p=0.0359$, *).

On the 13th day, it was observed that both the STD and EE+3 groups exhibited values above their respective baseline data, indicating noteworthy increases (Figure 28).

4.1.1.8 Left Steps Overlap Distance

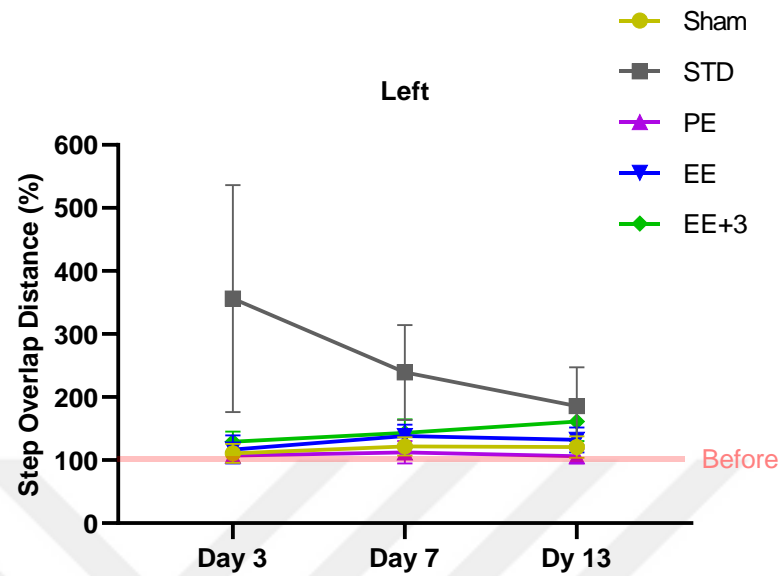


Figure 29. The left steps overlap distance across experimental groups in the footprint test analysis. Two Way repeated measure ANOVA TUKEY's multiple comparison test, *** $p < 0,001$, ** $p < 0,01$, * $p < 0,05$.

In the analysis of left steps overlap distance, no significant differences were observed either between the groups or within the groups over time (Figure 29)

Table 1. Footprint Test Results

Footprint Test Results				
Variables	Groups	Day 3	Day 7	Day 13
Right Hind Step Length	Sham vs. STD	P=0,0051 **	P=0,0535 ns	P= 0,4520 ns
	Sham vs. PE	P=0,0076 **	P=0,9298 ns	P >0,9999 ns
	Sham vs. EE	P=0,0094 **	P= 0,8745 ns	P= 0,9260 ns
	Sham vs. EE+3	P=0,0251 *	P=0,0016 *	P=0,0604 ns
Left Hind Step Length	Sham vs. EE +3	P=0,0088 **	P=0,0063 **	P= 0,0427 *
	Sham vs. EE	P= 0,1090 ns	P=0,0494 *	P= 0,3852 ns
Right Front Step Length	Sham vs. STD	P=0,0004 ***	P= 0,5156 ns	P= 0,9943 ns
	Sham vs. PE	P=0,0051 **	P= 0,9587 ns	P= 0,5848 ns
	Sham vs. EE	P=0,0495 *	P= 0,9886 ns	P= 0,9821 ns
	Sham vs. EE+3	P=0,0306 *	P= 0,0619 ns	P= 0,0915 ns
	PE vs. EE+3	p >0,9999 ns	P=0,0459 *	P=0,0271 *
Left Front Step Length	Sham vs. EE+3	P=0,0306 *	P= 0,0034 **	P= 0,0365 *
	PE vs. EE+3	P= 0,6558 ns	P= 0,0500 *	P= 0,0685 ns
	EE vs. EE+3	P= 0,3913 ns	P= 0,0265 *	P= 0,1308 ns
Right Step Overlap Distance	Sham vs. STD	P=0,0016 **	P= 0,3967 ns	P= 0,7764 ns
	STD vs. PE	P=0,0042 **	P= 0,2821 ns	P= 0,6484 ns
	STD vs. EE	P= 0,0175 *	P= 0,2917 ns	P= 0,7754 ns
	STD vs. EE+3	P=0,0446 *	P= 0,6089 ns	P= 0,9989 ns
	PE vs. EE+3	P= 0,9611 ns	P= 0,5868 ns	P= 0,0359 *

4.1.2. Wire Walk Test Analysis

4.1.2.1. Right Front Foot Fault

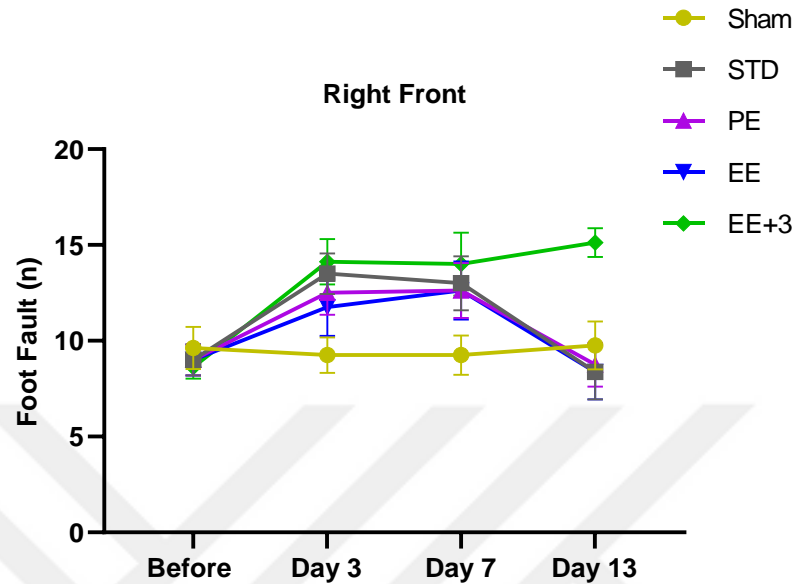


Figure 30. The right front foot fault across experimental groups in the wire walk test analysis. Two Way repeated measure ANOVA TUKEY's multiple comparison test, *** $p < 0,001$, ** $p < 0,01$, * $p < 0,05$.

On the 3rd day after injection, all groups except the sham group showed an increasing trend in right forelimb step errors. This increase was statistically significant when compared to baseline data on the 3rd day in the STD ($p=0.0218$, *), PE ($p=0.0456$, *), and EE+3 ($p=0.0039$, **) groups. While this significance disappeared in the PE and STD groups in the following days, it continued to increase statistically significantly in the EE+3 group when compared to baseline data on the 7th day ($p=0.0131$, *) and the 13th day ($p=0.0022$, **).

On the 3rd day post-injection, intergroup comparisons revealed a statistically significant difference between the sham and EE+3 groups ($p=0.0416$, *). Furthermore, while the difference between the sham and STD groups was not statistically significant, it approached significance ($p=0.0581$, ns).

On the 13th day, all experimental groups except the EE+3 group remained close to their baseline values. Notably, comparisons between groups revealed statistical significance between EE+3 and the sham ($p=0.0224$, *), STD ($p=0.0112$, *), PE ($p=0.0040$, **), and

EE ($p=0.0112$, *) groups. These findings indicate significant differences between the EE+3 group and the other experimental groups (Figure 30).

4.1.2.2. Left Front Foot Fault

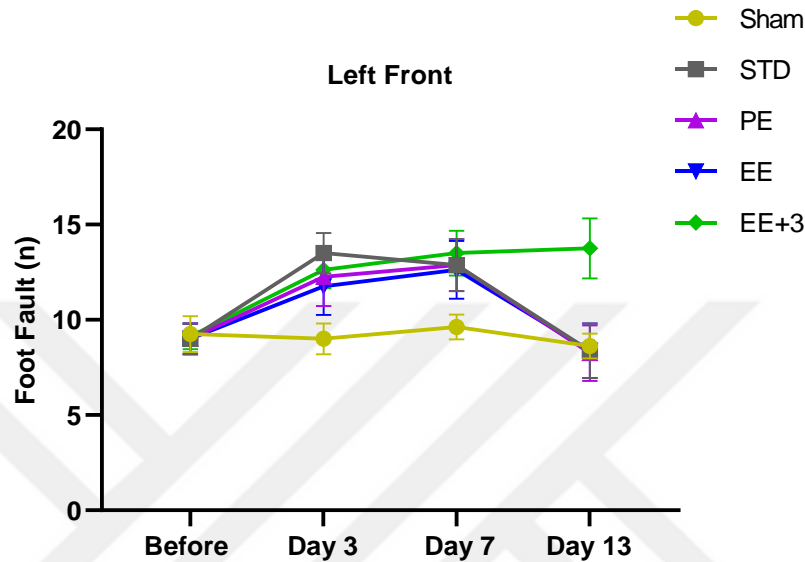


Figure 31. The left front foot fault across experimental groups in the wire walk test analysis. Two Way repeated measure ANOVA TUKEY's multiple comparison test, *** $p<0,001$, ** $p<0,01$, * $p<0,05$.

On the 3rd day after injection, an increasing trend in left front foot faults was observed in all groups except the sham group. When compared to baseline data, this increase was statistically significant in the STD ($p=0.0332$, *) and EE+3 ($p=0.0135$, *) groups. Additionally, on the 3rd day, intergroup comparisons revealed a statistically significant difference between the sham and STD groups ($p=0.0317$, *). On the 7th day, the increase in this variable in the STD group diminished but remained close to the threshold of significance ($p=0.0588$, ns). In contrast, the EE+3 group continued to show a statistically significant increase ($p=0.0070$, **).

On the 13th day, all groups, except for the EE+3 group, exhibited values approximating their baseline data. Conversely, the EE+3 group-maintained values above the baseline measurements (Figure 31 also see Table 2).

4.1.2.3. Right Hind Foot Fault

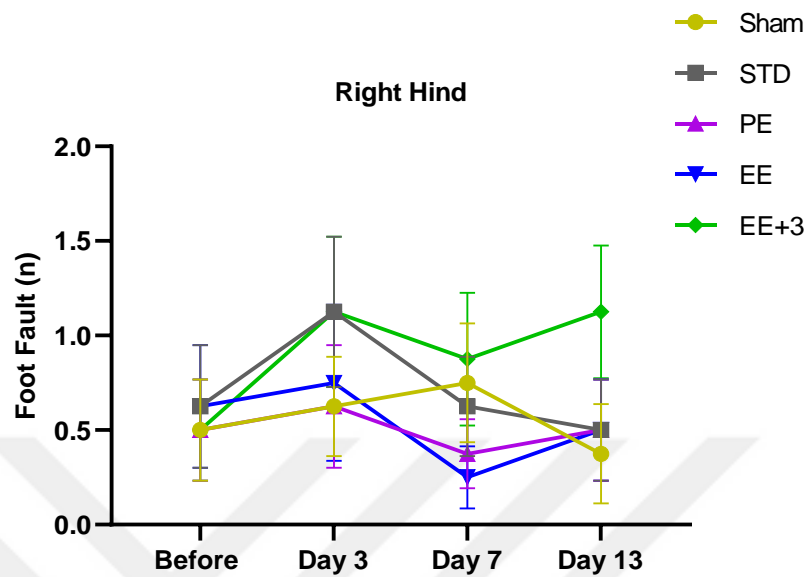


Figure 32. The right hind foot fault across experimental groups in the wire walk test analysis. Two Way repeated measure ANOVA TUKEY's multiple comparison test, *** $p < 0,001$, ** $p < 0,01$, * $p < 0,05$.

In the analysis of foot fault in the right hind limbs, no significant differences were found either between the groups or within the groups over time (Figure 32).

4.1.2.4. Left Hind Foot Fault

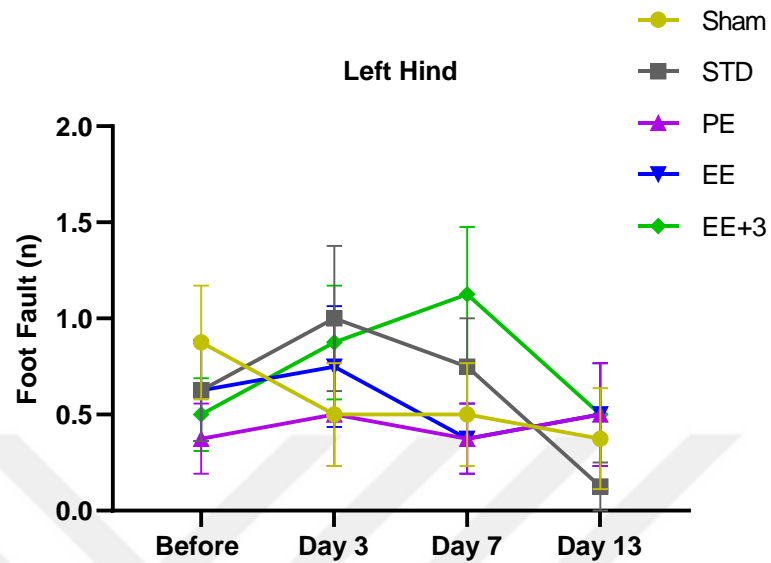


Figure 33. The left hind foot fault across experimental groups in the wire walk test analysis. Two Way repeated measure ANOVA TUKEY's multiple comparison test, *** $p < 0,001$, ** $p < 0,01$, * $p < 0,05$.

In the examination of left hind limb foot faults, no significant differences were detected either among the groups or within the groups over the period (Figure 33).

Table 2. Wire Walk Test Results

Wire Walk Test Results				
Variable	Groups	Day 3	Day 7	Day 13
Right Front Foot Fault	Sham vs. STD	P= 0,0581 ns	P= 0,2609 ns	P= 0,9470 ns
	Sham vs. EE+3	P=0,0416 *	P= 0,1701 ns	P= 0,0224 *
	STD vs. EE+3	P= 0,9943 ns	P= 0,9897 ns	P= 0,0112 *
	PE vs. EE+3	P= 0,8583 ns	P= 0,9678 ns	P= 0,0040 **
	EE vs. EE+3	P= 0,7243 ns	P= 0,9702 ns	P= 0,0112 *
Left Front Foot Fault	Sham vs. STD	P=0,0317 *	P= 0,2746 ns	P= 0,9998 ns

4.1.3. Three Chamber Test Analysis

4.1.3.1. Sociability (Part 1) Findings

The SPI for all groups was analyzed with two-way repeated measures ANOVA followed by Tukey's multiple comparison test. No significant differences were detected either among the groups or within the groups over the period (Figure 34).

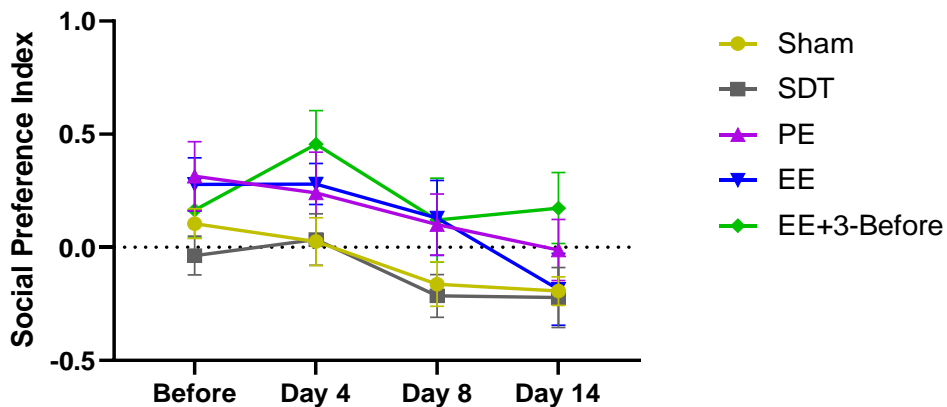


Figure 34. Social Preference Index. Two Way repeated measure ANOVA TUKEY's multiple comparison test, ***p<0,001, **p<0,01, *p<0,05.

4.1.3.2. Novelty (Part 2) Findings

The SNPI for all groups was analyzed with two-way repeated measures ANOVA followed by Tukey's multiple comparison test (Figure 35). Following the injection, a decreasing trend in SNPI values was observed in all groups except the sham group by day 4, with the EE+3, EE, and PE groups falling below the value of 0. However, after day 4, the groups that initially exhibited a decreasing trend began to show an increasing trend. This increasing trend became statistically significant on day 8 in the EE group when compared to baseline data ($p=0.0367$, *) and to day 4 data ($p=0.0112$, *). Additionally, in the PE group, this increase was statistically significant on day 14 when compared to day 4 data ($p=0.0156$, *). No significant differences were observed among the groups when comparisons were made.

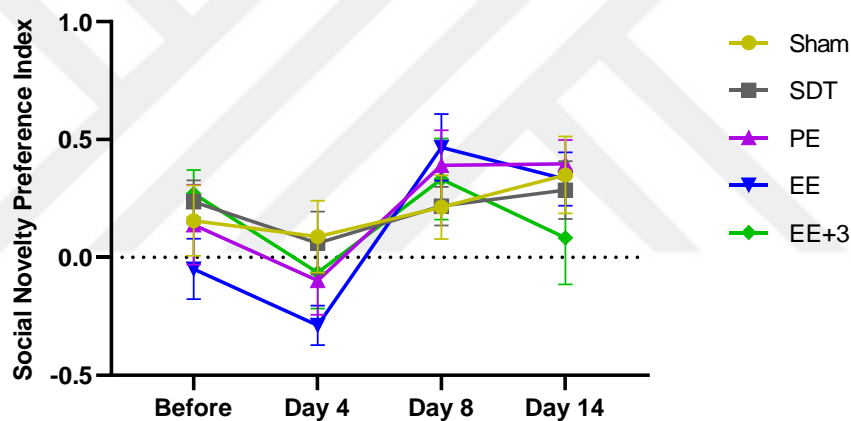


Figure 35. Social Novelty Preference Index. Two Way repeated measure ANOVA TUKEY's multiple comparison test, *** $p<0,001$, ** $p<0,01$, * $p<0,05$.

4.1.4. H&E Staining Findings

In the CI modeled SDT, PE, EE, and EE+3 groups, the results of H&E staining revealed that the injections successfully induced infarction in the target region. The corresponding alterations in anatomical structure are depicted in detail in Figure 36A.

A-) Cerebellar Infarction Model

B-) Reference Brain Section

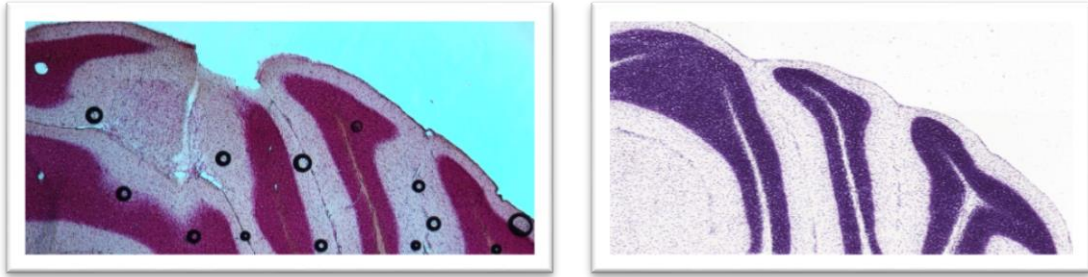


Figure 36. **A** represents a detailed modeling of CI using the H&E staining technique. **B**, on the other hand, provides an illustration of the target region of the cerebellum, detailed with a Reference Brain Section image obtained from the Brain Allen Atlas (82).

4.1.5 BOD1 Immunofluorescence Staining Findings

In the PE, EE, and EE+3 groups, an increase in BOD1 expression was observed within groups. This overexpression was not observed in the Sham and STD groups (Figure 37).

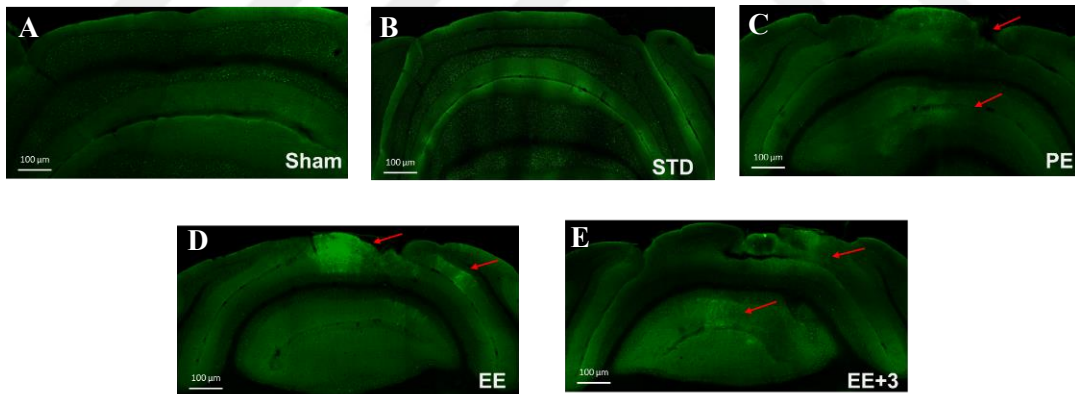


Figure 37. BOD1 immunofluorescence staining findings. Red arrows indicate regions with increased expression.

5. DISCUSSION

In the study, the CI model was induced using N5-(1-Iminoethyl)-L-ornithine dihydrochloride through stereotaxic injection. This substance, which narrows blood vessels, has been successfully used in past stroke models (83). Other methods to induce similar brain injuries include the injection of endothelin-1 into the brain, ligation of the anterior choroidal artery, and the use of L-NAME (84; 85). Endothelin-1 administration can result in unpredictable infarct sizes. When used in combination with L-NAME, infarcts typically form, but these infarcts tend to be smaller than expected and their sizes can vary across different species (86). Some studies show that L-NAME might protect the brain from ischemic damage (87; 88). Based on these findings, N5-(1-Iminoethyl)-L-ornithine dihydrochloride was selected as the method to induce ischemic lesions in the study. The successful induction of the CI modeling was confirmed by the results of the H&E staining.

The effects of the cerebellum on motor control may differ between the right and left hemispheres. The ipsilateral control characteristics of the cerebellum can directly influence the motor functions of the side where the damage occurs. Therefore, an injury to the right side of the cerebellum can lead to motor dysfunction on the right side of the body, depending on the topographically affected area and the severity of the damage. This dysfunction can manifest, for example, as impairments in motor function in the right forelimb and/or hindlimb. (89). The findings of the footprint test analysis in this study have demonstrated significant reductions in the step lengths of both the front and hind limbs on the right side. These findings are also consistent with gait analysis studies conducted on patients with cerebellar ataxia. For instance, Morton and Bastian (2004) demonstrated pronounced abnormalities in gait symmetry and step lengths in individuals with cerebellar damage (90). The reduction trend in step lengths was observed on the left side; however, these changes were not statistically significant. Right-sided cerebellar damage can affect not only the ipsilateral side but also the overall coordination of the body. This impairment can result in gait pattern asymmetry and reduced step lengths on the left side. Additionally, deficits on the right side can disrupt balance and symmetry, which may lead to adaptive or compensatory changes on the left side as well. Consequently, the asymmetric effects of cerebellar damage extend beyond localized areas, significantly impacting motor functions on the contralateral side (91).

The analysis of step widths did not reveal any significant differences, suggesting that the induced CI model has a limited impact on this specific gait parameter. Alternatively, other neuromuscular mechanisms may be working to stabilize step width. This may indicate that the body might employ alternative strategies to maintain balance and postural control, even when cerebellar damage impacts other aspects of gait (92; 93; 94).

The statistically significant increase in the step overlap distance of both the right front and hind limb steps indicates impairment in motor functions on the right side. On the other hand, an increase was also observed on the left side, but this was not found to be statistically significant. These findings further support the asymmetric effects of cerebellar damage and the complexity of reciprocal interactions (95; 96).

The wire walk test results showed a significant rise in foot faults for both the right and left forelimbs after inducing a CI model. This highlights the cerebellum's key role in motor planning and execution, especially for precise and coordinated movements (97). The increase in foot faults is particularly prominent in the right forelimb, aligning with the topographical mapping of the damaged cerebellar area (22). This direct mapping makes the observed motor impairment in the right forelimb expected, underscoring the cerebellum's specific influence on motor control (98). Interestingly, the observed significant increase in foot faults in the left forelimb indicates potential compensatory mechanisms or cross-hemispheric effects of cerebellar damage. This highlights the complexity of cerebellar influence on motor function. (99). On the other hand, no statistically significant difference was found in hindlimb foot faults. These findings may suggest that while mice use their hindlimbs primarily for stability, their forelimbs play a more critical role in managing fine motor skills and exploratory behaviors. Mice extensively use their forelimbs to interact with their environment, which requires complex and precise movements dependent on proper cerebellar function. Consequently, this may result in a higher incidence of errors observed in the forelimbs (100; 101).

It has been found that cerebellar lobule IV/V is more engaged in somatomotor tasks, while lobule IX is more involved during social interactions. (34). In this context, it is reasonable that the CI model did not show a significant difference in the three-chamber sociability test compared to the sham group (81). Additionally, it is known that perturbation of lobules IV/V does not evoke anxiety behavior, suggesting that social interactions in mice may remain unaffected (30). However, a stroke modeling study using N-methyl-D-

aspartate indicated an association between cerebellar lobule IV/V and social interactions (25). This contradiction suggests that the effects of cerebellar lobule IV/V on social behaviors may vary depending on experimental conditions and the characteristics of the model used. Therefore, it is understood that research using different models and methods is important to better understand the roles of cerebellar regions in social interactions.

The findings of the three-chamber social novelty preference test indicate that CI results in a decreasing trend in novelty-seeking behavior, suggesting impairments in cognitive functions such as novelty detection and preference. Although traditionally linked to motor control, the cerebellum is now recognized for its vital role in cognitive processes including attention, executive function, and novel stimulus processing (102). Additionally, the observed declining trend in novelty-seeking may reflect a negative impact on social recognition and memory, as these processes depend on the cerebellum's ability to integrate sensory inputs and process new information (103; 34).

EE is considered a promising new candidate factor in stroke treatment and rehabilitation management. This approach aims to enhance recovery by providing patients with a wide range of physical, social, cognitive, and sensory stimuli (104). Researches involving both rodents (105) and humans (106; 107) have shown that EE offers significant benefits in the recovery of motor skills, improvement of cognitive functions, and overall neurological recovery. However, the enrichment protocols are not well-defined, and it remains unclear which type of enrichment has the most significant impact on recovery. In this study, the effects of different types of enriched environmental conditions on motor and social performance were investigated. The findings have the potential to clarify which components of enriched environmental conditions are more effective on CI model mice. Additionally, it is important to highlight that the study offers an innovative approach by investigating the effects of enrichment applications on the CI model for the first time.

Based on the findings of the footprint test for PE group, it was determined that PE had a significant and positive effect on motor functions in CI model mice. Specifically, the motor dysfunction observed on the 3rd day showed significant improvements by the 7th and 13th days. The findings strongly supported that PE interventions are an effective method for recovery of motor dysfunction. Additionally, these findings align with research on the benefits of environmental enrichment for neurological recovery. Studies such as those by Bondi et al. (2014) have shown that PE can improve motor functions in

rodent models, which are linked to increased neuroplasticity and elevated levels of neurotrophic factors such as Brain-Derived Neurotrophic Factor (105). Furthermore, based on the findings of the wire walk test and in comparison, with the sham group data, it was observed that the PE group exhibited a faster recovery compared to the STD group. This also indicates that PE positively impacts motor functions. Lastly, the significant increase in SNPI values on day 13 compared to day 3 may suggest that PE positively influences cognitive processes such as social recognition and memory. Collectively, these results underscore the potential of PE as a therapeutic strategy for enhancing both motor and cognitive functions in CI model mice.

The components of the enrichment for the EE group consist of the same used in the PE group and the social enrichment, which is achieved by increasing the number of mice through co-housing CI model mice in the same cage. Accordingly, the effects of social enrichment conducted with CI model mice on motor and social performance were intended to be observed. Based on the findings from the footprint and wire walk tests, it was determined that the EE group exhibited recovery in their motor performance starting from day 3 and continuing through day 13. Specifically, the observation that the right step overlap distances in the EE group did not differ significantly from the sham group after injection on day 3 is notable. Additionally, it did show a significant difference from the STD group. This suggests that environmental conditions may help reduce the effects of damage on motor function even in the early stages. According to the results of the three-chamber test, it is noteworthy that SNPI values significantly increased, demonstrating a significant elevation even compared to the baseline data on day 8. This suggests that the exposed environmental conditions may positively influence intellectual processes such as social recognition and memory functions. Upon comparison with the PE group, the EE group did not exhibit a statistically significant difference in the measured outcomes. This suggests that the additional environmental enrichments provided to the EE group did not lead to significantly improved results compared to the physically enriched setting alone in the PE group. In this regard, increasing the number of CI model mice for social enrichment did not significantly impact motor performance and cognitive processes related to sociality.

The enrichment components for the EE+3 group consist of the same physical and social stimuli used in the EE group, with the addition of three healthy mice as an extra social enrichment component. Interestingly, based on the footprint and wire walk test results,

this group exhibited significant deficits in motor functions rather than recovery over time. Notably, according to the findings of the right front foot fault variable in the wire walk test, the EE+3 group showed a significant increase compared to all other experimental groups. Based on these findings, it is suggested that CI model mice experienced a negative impact on motor function when housed with healthy mice. This adverse effect may be attributed to the increased levels of stress and competition (108) introduced by the presence of healthy mice in the same environment. These conditions can create a more challenging and competitive landscape, potentially hindering the CI model mice's ability to recover and improve their motor function effectively. This hypothesis aligns with previous research indicating that stress (109) and competition in social environments can have a negative impact on neural and motor functions (110). Additionally, the EE+3 group did not exhibit significant changes in SNPI values over time, in contrast to the PE and EE groups. However, no statistical difference was found between the experimental groups. The inclusion of only three healthy mice may have been insufficient to produce a detectable impact. Increasing the sample size, particularly by introducing more healthy mice, could potentially provide clearer and more definitive results. By expanding the number of healthy mice, the effects of social enrichment may become more pronounced, allowing for a more accurate and robust assessment of its impact on SNPI values and other evaluated components.

Considering recent insights into the pathological mechanisms underlying cerebellar ataxia (73), our study's findings reveal a notable increase in BOD1 expression within the PE, EE, and EE+3 groups, while such overexpression was absent in the Sham and STD groups. The observed upregulation of BOD1 in specific experimental conditions may point towards an adaptive response that could be utilized for therapeutic intervention. Targeting BOD1 or its downstream signaling pathways might offer a promising avenue for developing treatments for cerebellar ataxia, highlighting the potential for translational research in this area to reduce the impact of this condition. However, our study has several limitations that future research should address. Firstly, while we observed an increase in BOD1 expression within the PE, EE, and EE+3 groups, we did not compare the levels of overexpression between these groups, which could provide deeper insights into the relative effects of different environmental enrichments. Furthermore, the experimental groups might not fully capture the complexity and variability of cerebellar ataxia in human patients, indicating a need for additional models and larger sample sizes to validate

our findings. Lastly, future studies need to evaluate whether modulation of BOD1 expression induces any off-target effects and to assess the long-term safety and efficacy of such therapeutic strategies *in vivo*.

In conclusion, this study highlights the critical importance of intervention type in promoting motor recovery after CI. The results indicate that PE and EE are particularly effective for enhancing motor function and positively affecting cognitive processes. In contrast, social enrichment with healthy mice was linked to sustained motor deficits, suggesting it might not offer the same benefits. The increased BOD1 expression observed in the PE, EE, and EE+3 groups suggest a response that could be leveraged for therapeutic strategies against cerebellar ataxia. However, further research is needed to compare expression levels among these groups, explore additional models, and assess the long-term safety and efficacy of targeting BOD1.

6. REFERENCES

1. Datar, S., & Rabinstein, A. A. Cerebellar infarction. *Neurologic clinics*. 2014;32(4), 979-991. doi:10.1016/j.ncl.2014.07.007.
2. Prasad A, Nookala V, Machchar R, Simon JR, Nakka LA, Vanamala T, et al. Predictors of Outcomes in Cerebellar Stroke: A Retrospective Cohort Study From the National Inpatient Sample Data. *Cureus*. 2024;16(6). doi:10.7759/cureus.62025.
3. Edlow, J. A., Newman-Toker, D. E., & Savitz, S. I. Diagnosis and initial management of cerebellar infarction. *The Lancet Neurology*. 2008;7(10), 951-964. doi:10.1016/S1474-4422(08)70216-3.
4. Stoodley, C. J., & Schmahmann, J. D. Evidence for topographic organization in the cerebellum of motor control versus cognitive and affective processing. *Cortex*. 2010;46(7), 831-844. doi: 10.1016/j.cortex.2009.11.008.
5. Gorlamandala N, Parmar J, Craig AJ, Power JM, Moorhouse AJ, Krishnan A V., et al. Focal Ischaemic Infarcts Expand Faster in Cerebellar Cortex than Cerebral Cortex in a Mouse Photothrombotic Stroke Model. *Translational stroke research*. 2018 Dec 1;9(6):643–53. doi: 10.1007/S12975-018-0615-1.
6. Marsden, J., & Harris, C. Cerebellar ataxia: pathophysiology and rehabilitation. *Clinical rehabilitation*. 2012;25(3), 195-216. doi:10.1177/0269215510382495.
7. Sharma, R., Romi, S. N., & Srivastava, R. K. An objective approach for assessment of balance disorders and role of visual biofeedback training in the treatment of balance disorders: A preliminary study. *IJPMR*. 2001;12, 25-30.
8. Karakaya, M., Kose, N., Otman, S., Ozgen, T., & Papo, I. (2000). Investigation and comparison of the effects of rehabilitation on balance and coordination problems in patients with posterior fossa and cerebellopontine angle tumours. *Journal of Neurosurgical Sciences*. 2000;44(4), 220.

9. Manto, M., Godaux, E., & Jacquy, J. Cerebellar hypermetria is larger when the inertial load is artificially increased. *Annals of Neurology: Official Journal of the American Neurological Association and the Child Neurology Society*. 1994;35(1),45-52.
10. Mellen, J., & Sevenich MacPhee, M. Philosophy of environmental enrichment: past, present, and future. *Zoo Biology*.2001;20(3), 211-226. doi:10.1002/zoo.1021.
11. Yu K, Wu Y, Zhang Q, Xie H, Liu G, Guo Z, et al. Enriched environment induces angiogenesis and improves neural function outcomes in rat stroke model. *Journal of the neurological sciences*. 2014;347(1-2), 275-280. doi:10.1016/j.jns.2014.10.022.
12. Janssen H, Ada L, Bernhardt J, Mcelduff P, Pollack M, Nilsson M, et al. An enriched environment increases activity in stroke patients undergoing rehabilitation in a mixed rehabilitation unit: a pilot non-randomized controlled trial. *Disability and rehabilitation*. 2014;36(3), 255-262. doi: 10.3109/09638288.2013.788218.
13. Gelfo, F., & Petrosini, L. Environmental enrichment enhances cerebellar compensation and develops cerebellar reserve. *International Journal of Environmental Research and Public Health*. 2022;19(9), 5697. doi:10.3390/ijerph19095697
14. Suckow, M. A., & Stewart, K. Principles of animal research for graduate and undergraduate students. Academic Press. 2016
15. Balıkcı, A. Exploring Effects of the HEP (Homeostasis-Enrichment-Plasticity) Approach as a Comprehensive Therapy Intervention for an Infant with Cerebral Palsy: A Case Report. *Journal of Child Science*. 2022;12(01), e182-e195. doi:10.1055/s-0042-1757913
16. Hawkes, R. B. *Cerebellum: Anatomy and Organization*. eLS. 2001. doi:10.1038/NPG.ELS.0004071

17. Ozol, K., Hayden, J. M., Oberdick, J., & Hawkes, R. Transverse zones in the vermis of the mouse cerebellum. *Journal of Comparative Neurology*. 1999;412(1), 95-111. doi:10.1002/(SICI)1096-9861(19990913)412:1<95::AID-CNE7>3.0.CO;2-Y
18. Apps, R., & Hawkes, R. Cerebellar cortical organization: a one-map hypothesis. *Nature Reviews Neuroscience*. 2009;10(9), 670-681.
19. D'Mello, A. M., & Stoodley, C. J. Cerebro-cerebellar circuits in autism spectrum disorder. *Frontiers in neuroscience*. 2015;9, 408. doi:10.3389/FNINS.2015.00408/FULL.
20. Voogd, J., & Ruigrok, T. J. The organization of the corticonuclear and olivocerebellar climbing fiber projections to the rat cerebellar vermis: the congruence of projection zones and the zebrin pattern. *Journal of neurocytology*. 2004;33(1), 5-21. doi:10.1023/B:NEUR.0000029645.72074.2B.
21. Sotelo, C., & Chédotal, A. Development of the olivocerebellar system: migration and formation of cerebellar maps. *Progress in brain research*. 2005;148, 1-20.
22. Diedrichsen, J., & Zotow, E. Surface-based display of volume-averaged cerebellar imaging data. *PloS one*. 2015;10(7),e0133402. doi:10.1371/journal.pone.0133402.
23. Buckner, R. L., Krienen, F. M., Castellanos, A., Diaz, J. C., & Yeo, B. T. The organization of the human cerebellum estimated by intrinsic functional connectivity. *Journal of neurophysiology*. 2011;106(5), 2322-2345. doi:10.1152/jn.00339.2011
24. Grodd, W., Hülsmann, E., Lotze, M., Wildgruber, D., & Erb, M. (2001). Sensorimotor mapping of the human cerebellum: fMRI evidence of somatotopic organization. *Human brain mapping*. 2001;13(2), 55-73. doi: 10.1002/hbm.1025
25. Chao, O. Y., Zhang, H., Pathak, S. S., Huston, J. P., & Yang, Y. M. Functional convergence of motor and social processes in lobule IV/V of the mouse cerebellum. *The Cerebellum*. 2021;1-17. doi: 10.1007/S12311-021-01246-7

26. Shunkai L, Su T, Wang Y, Zhong S, Chen G, Zhang Y, et al. Abnormal dynamic functional connectivity of hippocampal subregions associated with working memory impairment in melancholic depression. *Psychological medicine*. 2023;53(7), 2923-2935. doi:10.1017/S0033291721004906.
27. Zeidler, Z., Hoffmann, K., & Krook-Magnuson, E. HippoBellum: acute cerebellar modulation alters hippocampal dynamics and function. *Journal of Neuroscience*. 2020;40(36), 6910-6926. doi:10.1523/JNEUROSCI.0763-20.2020.
28. Adrian, E. D. Discharges from vestibular receptors in the cat. *The Journal of physiology*. 1943;101(4), 389.
29. Snider, R. S., & Stowell, A. Receiving areas of the tactile, auditory, and visual systems in the cerebellum. *Journal of Neurophysiology*. 1944;7(6), 331-357.
30. Chin, P. W., & Augustine, G. J. The cerebellum and anxiety. *Frontiers in Cellular Neuroscience*. 2023;17, 1130505. doi:10.3389/fncel.2023.1130505.
31. Iglói K, Doeller CF, Paradis A-L, Benchenane K, Berthoz A, Burgess N, et al. Interaction between hippocampus and cerebellum crus I in sequence-based but not place-based navigation. *Cerebral Cortex*. 2015;25(11), 4146-4154.
32. Van Overwalle F, Manto M, Cattaneo Z, Clausi S, Ferrari C, Gabrieli JDE, et al. Consensus paper: cerebellum and social cognition. *The Cerebellum*. 2020;19, 833-868. doi:10.1007/s12311-020-01155-1
33. Van Overwalle, F., Baetens, K., Mariën, P., & Vandekerckhove, M. Social cognition and the cerebellum: a meta-analysis of over 350 fMRI studies. *Neuroimage*. 2014;86, 554-572.
34. Van Overwalle F, Manto M, Cattaneo Z, Clausi S, Ferrari C, Gabrieli JDE, et al. Consensus paper: cerebellum and social cognition. *The Cerebellum*. 2020;19, 833-868. doi: 10.1007/s12311-020-01155-1
35. Icardo, J. M., Ojeda, J. L., Garcia-Porrero, J. A., & Hurle, J. M. The cerebellar arteries: cortical patterns and vascularization of the cerebellar nuclei. *Cells Tissues Organs*. 1982;113(2), 108-116.
36. De Cocker, L. J., Geerlings, M. I., Hartkamp, N. S., et al. Cerebellar infarct patterns: the SMART-Medea study. *NeuroImage: Clinical*. 2015;8, 314-321.

37. De Cocker, L. J., Lövblad, K. O., & Hendrikse, J. MRI of cerebellar infarction. *European Neurology*. 2017;77(3-4), 137-146.
38. Stoodley, C. J., & Schmahmann, J. D. Evidence for topographic organization in the cerebellum of motor control versus cognitive and affective processing. *cortex*. 2010;46(7), 831-844.
39. Peng S, Liu X, Cao W, Liu Y, Liu Y, ... WW-IJ of, et al. Global, regional, and national time trends in mortality for stroke, 1990–2019: An age-period-cohort analysis for the global burden of disease 2019 study and implications for stroke prevention. *International Journal of Cardiology*. 2023;383, 117-131.
40. Lozano, R., Naghavi, M., Foreman, K., Lim, S., Shibuya, K., et al. Global and regional mortality from 235 causes of death for 20 age groups in 1990 and 2010: a systematic analysis for the Global Burden of Disease Study 2010. *The lancet*. 2012;380(9859), 2095-2128.
41. Fan J, Li X, Yu X, Liu Z, Jiang Y, Fang Y, et al. Global burden, risk factor analysis, and prediction study of ischemic stroke, 1990–2030. *Neurology*. 2023;101(2), e137-e150. doi:10.1212/WNL.0000000000207387.
42. World Health Organization. Burden of diseases statistics. Geneva, Switzerland: World Health Organization. Available at: <https://www.emro.who.int/health-topics/stroke-cerebrovascular-accident/index.html> (accessed May 21, 2024).
43. Feigin V, Abajobir A, Abate K., et all. Global, regional, and national burden of neurological disorders during 1990–2015: a systematic analysis for the Global Burden of Disease Study 2015. *The Lancet Neurology*. 2017;16(11), 877-897.
44. Lavados P, Sacks C, Prina L, Escobar A, et all. Incidence, 30-day case-fatality rate, and prognosis of stroke in Iquique, Chile: a 2-year community-based prospective study (PISCIS project). *The Lancet*. 2005;365(9478), 2206-2215.
45. Calic Z, Cappelen-Smith C, et all. Frequency, aetiology, and outcome of small cerebellar infarction. *Cerebrovascular diseases extra*. 2018;7(3), 173-180.
46. Feigin, V. L., Lawes, C. M., Bennett, D. A., & Anderson, C. S. Stroke epidemiology: a review of population-based studies of incidence, prevalence, and case-fatality in the late 20th century. *The lancet neurology*. 2003;2(1), 43-53.

47. Tohgi, H., Takahashi, S., Chiba, K., & Hirata, Y. Cerebellar infarction. Clinical and neuroimaging analysis in 293 patients. The Tohoku cerebellar infarction study Group. *Stroke*. 1993;24(11), 1697-1701.
48. Macdonell, R. A., Kalnins, R. M., & Donnan, G. A. Cerebellar infarction: natural history, prognosis, and pathology. *Stroke*. 1987;18(5), 849-855.
49. Kase CS, Norrving B, Levine SR, Babikian VL, Chodosh EH, Wolf PA, et al. Cerebellar infarction clinical and anatomic observations in 66 cases. *Stroke*. 1993;24(1):76–83.
50. Timmann, D., & Daum, I. Cerebellar contributions to cognitive functions: a progress report after two decades of research. *The cerebellum*. 2007;6, 159-162.
51. Schmahmann, J. D. Disorders of the cerebellum: ataxia, dysmetria of thought, and the cerebellar cognitive affective syndrome. *The Journal of neuropsychiatry and clinical neurosciences*. 2004;16(3), 367-378.
52. Schmahmann, J. D., & Sherman, J. C. The cerebellar cognitive affective syndrome. *Brain: a journal of neurology*. 1998;121(4), 561-579.
53. Brandt, L., Liu, S., Heim, C., & Heinz, A. The effects of social isolation stress and discrimination on mental health. *Translational psychiatry*. 2022;12(1), 398.
54. Langhorne, P., Bernhardt, J., & Kwakkel, G. Stroke rehabilitation. *The Lancet*. 2011;377(9778), 1693-1702.
55. Amarenco, P., Levy, C., Cohen, A., Touboul, P. J., Roullet, E., & Bousser, M. G. Causes and mechanisms of territorial and nonterritorial cerebellar infarcts in 115 consecutive patients. *Stroke*. 1994;25(1), 105-112.
56. Amarenco P. The spectrum of cerebellar infarctions. *Neurology*. 1991;41(7):973–9.
57. Amarenco P, Hauw J-J. Cerebellar infarction in the territory of the superior cerebellar artery. *Neurology*. 1990 Sep;40(9):1383–1383.

58. Lip GYH, Lane DA, Lenarczyk R, Boriani G, Doehner W, Benjamin LA, et al. Integrated care for optimizing the management of stroke and associated heart disease: a position paper of the European Society of Cardiology Council on Stroke. *European Heart Journal*. 2022;43(26), 2442-2460.
59. Marsden, J., & Harris, C. Cerebellar ataxia: pathophysiology and rehabilitation. *Clinical rehabilitation*. 2011;25(3), 195-216.
60. Sharma, R., Romi, S. N., & Srivastava, R. K. An objective approach for assessment of balance disorders and role of visual biofeedback training in the treatment of balance disorders: A preliminary study. *IJPMR*. 2001;12, 25-30.
61. Karakaya, M., Kose, N., Otman, S., Ozgen, T., & Papo, I. (2000). Investigation and comparison of the effects of rehabilitation on balance and coordination problems in patients with posterior fossa and cerebellopontine angle tumours. *Journal of Neurosurgical Sciences*. 2000;44(4), 220.
62. Veldema, J., & Jansen, P. Resistance training in stroke rehabilitation: systematic review and meta-analysis. *Clinical rehabilitation*. 2020;34(9), 1173-1197.
63. Mellen, J., & Sevenich MacPhee, M. Philosophy of environmental enrichment: past, present, and future. *Zoo Biology*. 2001;20(3), 211-226.
64. Nithianantharajah, J., & Hannan, A. J. Enriched environments, experience-dependent plasticity and disorders of the nervous system. *Nature Reviews Neuroscience*. 2006;7(9), 697-709.
65. Ohlsson AL, Johansson BB. Environment influences functional outcome of cerebral infarction in rats. *Stroke*. 1995;26(4):644-9.
66. Rönnbäck, A., Dahlqvist, P., Svensson, P. A., Jernås, M., Carlsson, B., Carlsson, L. M., & Olsson, T. Gene expression profiling of the rat hippocampus one month after focal cerebral ischemia followed by enriched environment. *Neuroscience letters*. 2005;385(2), 173-178.
67. Yu, K, Wu, Y, Zhang, Q, Xie, H, Liu, G, Guo, Z, et all. Enriched environment induces angiogenesis and improves neural function outcomes in rat stroke model. *Journal of the neurological sciences*. 2014;347(1-2), 275-280.

68. Nithianantharajah, J., & Hannan, A. J. Enriched environments, experience-dependent plasticity and disorders of the nervous system. *Nature Reviews Neuroscience*. 2006;7(9), 697-709.
69. Morgan, C., Novak, I., & Badawi, N. Enriched environments and motor outcomes in cerebral palsy: systematic review and meta-analysis. *Pediatrics*. 1013;132(3), e735-e746.
70. Ball, N. J., Mercado III, E., & Orduña, I. Enriched environments as a potential treatment for developmental disorders: a critical assessment. *Frontiers in psychology*. 2019;10, 466.
71. Rogers, S. J., Hepburn, S., & Wehner, E. Parent reports of sensory symptoms in toddlers with autism and those with other developmental disorders. *Journal of autism and developmental disorders*. 2003;33, 631-642.
72. Troschel FM, Bö Hly N, Borrmann K, Braun T, Schwickert A, Kiesel L, et al. miR-142-3p attenuates breast cancer stem cell characteristics and decreases radioresistance in vitro. *tumor biology*. 2018;40(8), 1010428318791887.
73. Liu X-X, Chen X-H, Zheng Z-W, Jiang Q, Li C, Yang L, et al. BOD1 regulates the cerebellar IV/V lobe-fastigial nucleus circuit associated with motor coordination. *Signal Transduction and Targeted Therapy*. 2022;7(1), 170.
74. Carlson ES, Hunker AC, Sandberg SG, Locke TM, Geller JM, Schindler AG, et al. Catecholaminergic innervation of the lateral nucleus of the cerebellum modulates cognitive behaviors. *Neuroscience*. 2021;41(15), 3512-3530.
75. Sun, H., & Wang, G. Local Circuits in the Cerebellum Interact with Biochemical Events. *Neuroscience Bulletin*. 2023;39(4), 710-712.
76. Aykan Dilmen SA. The Effect Of Rho-Kinase Inhibitors In Focal Cerebellar Infarct Mouse Model. Ankara. Hacettepe University Institute Of Health Sciences, 2018.
77. Brooks, S. P., Trueman, R. C., & Dunnett, S. B. Assessment of motor coordination and balance in mice using the rotarod, elevated bridge, and footprint tests. *Current Protocols in Mouse Biology*. 2012;2(1), 37-53.

78. Rogers DC, Campbell CA, Stretton JL, Mackay KB. Correlation between motor impairment and infarct volume after permanent and transient middle cerebral artery occlusion in the rat. *Stroke*. 1997;28(10):2060–6.
79. Allred, R. P., & Jones, T. A. Maladaptive effects of learning with the less-affected forelimb after focal cortical infarcts in rats. *Experimental neurology*. 2008;210(1), 172-181.
80. Kaidanovich-Beilin, O., Lipina, T., Vukobradovic, I., Roder, J., & Woodgett, J. R. Assessment of social interaction behaviors. *JoVE (Journal of Visualized Experiments)*. 2011;(48), e2473.
81. Chao, O. Y., Pathak, S. S., Zhang, H., Augustine, G. J., Christie, J. M., Kikuchi, C., et al. Social memory deficit caused by dysregulation of the cerebellar vermis. *Nature communications*. 2023;14(1), 6007.
82. Allen Institute for Brain Science. Allen Mouse Brain Atlas. 2008. Available from: <https://mouse.brain-map.org/experiment/siv?id=100142143&imageId=102162054&imageType=atlas&initImage=atlas&showSubImage=y&contrast=0.5,0.5,0,255,4>
83. Hinman JD, Rasband MN, Carmichael ST. Remodeling of the axon initial segment after focal cortical and white matter stroke. *Stroke*. 2013 Jan;44(1):182–9.
84. Ahmad, A. S., Satriotomo, I., Fazal, J., Nadeau, S. E., & Dore, S. Considerations for the optimization of induced white matter injury preclinical models. *Frontiers in neurology*. 2015;6, 172.
85. Hughes, P. M., Anthony, D. C., Ruddin, M., Botham, M. S., Rankine, E. L., Sablone, et al. Focal lesions in the rat central nervous system induced by endothelin-1. *Journal of Neuropathology & Experimental Neurology*. 2003;62(12), 1276-1286.
86. Horie, N., Maag, A. L., Hamilton, S. A., Shichinohe, H., Bliss, T. M., & Steinberg, G. K. Mouse model of focal cerebral ischemia using endothelin-1. *Journal of neuroscience methods*. 2008;173(2), 286-290.

87. Ashwal, S., Cole, D. J., Osborne, S., Osborne, T. N., & Pearce, W. J. L-NAME reduces infarct volume in a filament model of transient middle cerebral artery occlusion in the rat pup. *Pediatric research*. 1995;38(5), 652-656.
88. Quast, M. J., Wei, J., & Huang, N. C. Nitric oxide synthase inhibitor NG-nitro-L-arginine methyl ester decreases ischemic damage in reversible focal cerebral ischemia in hyperglycemic rats. *Brain research*. 1995;677(2), 204-212.
89. Holmes, G. The cerebellum of man. *Brain*. 1939; 62(1), 1-30.
90. Morton, S. M., & Bastian, A. J. Cerebellar control of balance and locomotion. *The neuroscientist*. 2004 10(3), 247-259.
91. Ilg, W., & Timmann, D. Gait ataxia—specific cerebellar influences and their rehabilitation. *Movement disorders*. 2013;28(11), 1566-1575.
92. Morton, S. M., & Bastian, A. J. Cerebellar control of balance and locomotion. *The neuroscientist*. 2004;10(3), 247-259.
93. Horak, F. B., & Diener, H. C. Cerebellar control of postural scaling and central set in stance. *Journal of neurophysiology*. 1994;72(2), 479-493.
94. Morton, S. M., & Bastian, A. J. Cerebellar control of balance and locomotion. *The neuroscientist*. 2004;10(3), 247-259.
95. Doya, K. Complementary roles of basal ganglia and cerebellum in learning and motor control. *Current opinion in neurobiology*. 2000;10(6), 732-739.
96. Morton, S. M., & Bastian, A. J. Cerebellar contributions to locomotor adaptations during splitbelt treadmill walking. *Journal of Neuroscience*. 2006;26(36), 9107-9116.
97. Miterko, L. N., Baker, K. B., Beckinghausen, J., Bradnam, L. V., Cheng, M. Y., Cooperrider, J., et al. Consensus paper: experimental neurostimulation of the cerebellum. *The Cerebellum*. 2019;18, 1064-1097.
98. Ebner, T. J., Hewitt, A. L., & Popa, L. S. What features of limb movements are encoded in the discharge of cerebellar neurons?. *The cerebellum*. 2011;10, 683-693.

99. Boyle, G. J., Northoff, G., Barbey, A. K., Fregni, F., Jahanshahi, M., Pascual-Leone, A., & Sahakian, B. J. (Eds.). *The Sage Handbook of Cognitive and Systems Neuroscience: Cognitive Systems, Development and Applications*. SAGE Publications Limited. 2023.
100. Kleinfeld, D., & Deschênes, M. Neuronal basis for object location in the vibrissa scanning sensorimotor system. *Neuron*. 2011;72(3), 455-468.
101. Whishaw, I. Q., & Kolb, B. (Eds.). *The behavior of the laboratory rat: a handbook with tests*. Oxford university press. 2004
102. Buckner, R. L. The cerebellum and cognitive function: 25 years of insight from anatomy and neuroimaging. *Neuron*. 2013;80(3), 807-815.
103. Manto, M. The underpinnings of cerebellar ataxias. *Clinical neurophysiology practice*. 2022;7, 372-387.
104. McDonald, M. W., Hayward, K. S., Rosbergen, I. C., Jeffers, M. S., & Corbett, D. Is environmental enrichment ready for clinical application in human post-stroke rehabilitation?. *Frontiers in behavioral neuroscience*. 2018;12, 135.
105. Bondi, C. O., Klitsch, K. C., Leary, J. B., & Kline, A. E. Environmental enrichment as a viable neurorehabilitation strategy for experimental traumatic brain injury. *Journal of neurotrauma*. 2014;31(10), 873-888.
106. Rosbergen, I. C., Grimley, R. S., Hayward, K. S., Walker, K. C., Rowley, D., Campbell, A. M., et al. Embedding an enriched environment in an acute stroke unit increases activity in people with stroke: a controlled before–after pilot study. *Clinical rehabilitation*. 2017;31(11), 1516-1528.
107. White, J. H., Bartley, E., Janssen, H., Jordan, L. A., & Spratt, N. Exploring stroke survivor experience of participation in an enriched environment: a qualitative study. *Disability and rehabilitation*. 2015;37(7), 593-600.
108. Creel, S. Social dominance and stress hormones. *Trends in ecology & evolution*. 2001;16(9), 491-497.
109. Apazoglou, K., Mazzola, V., Wegrzyk, J., Polara, G. F., & Aybek, S. Biological and perceived stress in motor functional neurological disorders. *Psychoneuroendocrinology*. 2017;85, 142-150.

110. Gasser-Haas, O., Sticca, F., & Wustmann Seiler, C. Poor motor performance—do peers matter? Examining the role of peer relations in the context of the environmental stress hypothesis. *Frontiers in psychology*. 2020;11, 498.

